

Measurement of single top-quark production in association with a W boson in the single-lepton channel at $\sqrt{s} = 8\text{TeV}$ with the ATLAS detector

ATLAS Collaboration

DOI:

[10.1140/epjc/s10052-021-09371-7](https://doi.org/10.1140/epjc/s10052-021-09371-7)

License:

Creative Commons: Attribution (CC BY)

Document Version

Publisher's PDF, also known as Version of record

Citation for published version (Harvard):

ATLAS Collaboration 2021, 'Measurement of single top-quark production in association with a W boson in the single-lepton channel at $\sqrt{s} = 8\text{TeV}$ with the ATLAS detector', *Eur. Phys. J. C*, vol. 81, no. 8, 720.
<https://doi.org/10.1140/epjc/s10052-021-09371-7>

[Link to publication on Research at Birmingham portal](#)

General rights

Unless a licence is specified above, all rights (including copyright and moral rights) in this document are retained by the authors and/or the copyright holders. The express permission of the copyright holder must be obtained for any use of this material other than for purposes permitted by law.

- Users may freely distribute the URL that is used to identify this publication.
- Users may download and/or print one copy of the publication from the University of Birmingham research portal for the purpose of private study or non-commercial research.
- User may use extracts from the document in line with the concept of 'fair dealing' under the Copyright, Designs and Patents Act 1988 (?)
- Users may not further distribute the material nor use it for the purposes of commercial gain.

Where a licence is displayed above, please note the terms and conditions of the licence govern your use of this document.

When citing, please reference the published version.

Take down policy

While the University of Birmingham exercises care and attention in making items available there are rare occasions when an item has been uploaded in error or has been deemed to be commercially or otherwise sensitive.

If you believe that this is the case for this document, please contact UBIRA@lists.bham.ac.uk providing details and we will remove access to the work immediately and investigate.



Measurement of single top-quark production in association with a W boson in the single-lepton channel at $\sqrt{s} = 8$ TeV with the ATLAS detector

ATLAS Collaboration*

CERN, 1211 Geneva 23, Switzerland

Received: 6 July 2020 / Accepted: 23 June 2021
© CERN for the benefit of the ATLAS collaboration 2021

Abstract The production cross-section of a top quark in association with a W boson is measured using proton–proton collisions at $\sqrt{s} = 8$ TeV. The dataset corresponds to an integrated luminosity of 20.2 fb^{-1} , and was collected in 2012 by the ATLAS detector at the Large Hadron Collider at CERN. The analysis is performed in the single-lepton channel. Events are selected by requiring one isolated lepton (electron or muon) and at least three jets. A neural network is trained to separate the tW signal from the dominant $t\bar{t}$ background. The cross-section is extracted from a binned profile maximum-likelihood fit to a two-dimensional discriminant built from the neural-network output and the invariant mass of the hadronically decaying W boson. The measured cross-section is $\sigma_{tW} = 26 \pm 7 \text{ pb}$, in good agreement with the Standard Model expectation.

Contents

1	Introduction
2	ATLAS detector
3	Data and simulated event samples
4	Object definitions
5	Event selection
6	Separation of signal from background
6.1	Invariant mass of the hadronically decaying W boson
6.2	Neural network
6.3	Two-dimensional discriminant
7	Systematic uncertainties
8	Statistical analysis
9	Cross-section measurement
10	Conclusion
	References

* e-mail: atlas.publications@cern.ch

1 Introduction

Single top quarks are produced in proton–proton collisions via the weak interaction. At leading order (LO) three different channels, which depend on the virtuality of the W boson involved, are defined: t -channel, s -channel or top-quark production in association with a W boson, called tW production. These processes, for which example Feynman diagrams are shown in Fig. 1, involve a Wtb vertex at LO in the Standard Model (SM). Calculations involving tW production beyond LO have to include quantum interference with $t\bar{t}$ production. Measurements of single-top-quark cross-sections are used to study the properties of this vertex, as they are directly sensitive to the Cabibbo–Kobayashi–Maskawa (CKM) matrix element $|V_{tb}|$. Deviations from the cross-sections predicted by the SM can originate from single top quarks produced with similar kinematics in the decays of unknown heavy particles predicted by physics beyond the Standard Model. If the masses of these particles are beyond the reach of direct searches, they might be revealed through their effects on the effective Wtb coupling [1]. Using measurements in all three channels of single top-quark production, physics beyond the SM can be probed systematically in the context of Effective Field Theory [2]. As each of the single-top-quark processes can be sensitive to different sources of new physics, it is also important to study each channel separately. In addition, the SM production of tW is an important background in direct searches for particles beyond the SM [3,4].

At the Large Hadron Collider (LHC), evidence for the tW production process was found by the ATLAS [5] and CMS Collaborations [6] at $\sqrt{s} = 7$ TeV and the process was observed by both experiments [7,8] at $\sqrt{s} = 8$ TeV. The tW cross-section has been also measured with 13 TeV collision data inclusively by the CMS Collaboration [9] as well as inclusively and differentially by the ATLAS Collaboration [10–12]. These measurements were performed in final states with two leptons, and the measured cross-sections agree with the theoretical expectations.

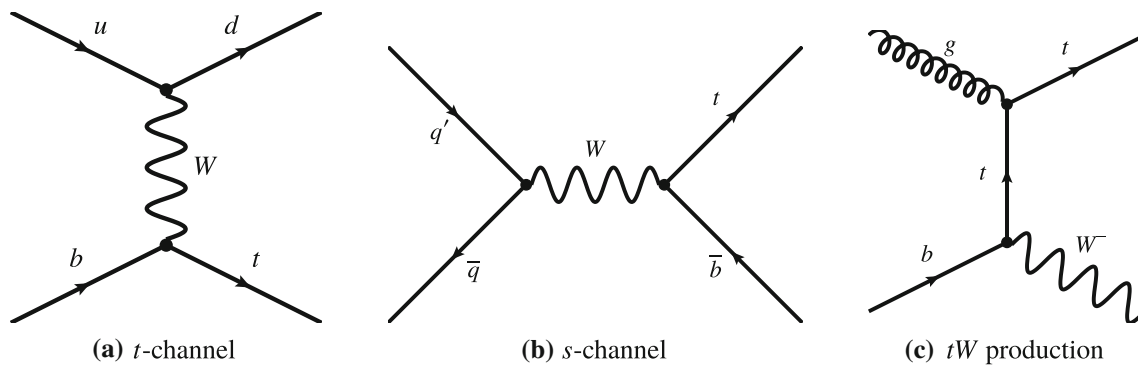


Fig. 1 Example LO Feynman diagrams of single top-quark production: **a** t -channel, **b** s -channel and **c** tW production

This paper presents evidence for tW production in final states with a single lepton using proton–proton (pp) collisions at $\sqrt{s} = 8$ TeV. This topology features a W boson in addition to a top quark, which decays mainly into another W boson and b -quark, leading to a W^+W^-b state. In the single-lepton channel, one of the W bosons decays leptonically (W_L) while the other one decays hadronically (W_H). Therefore, the experimental signature of event candidates is characterised by one isolated charged lepton (electron or muon), large missing transverse momentum (E_T^{miss}), and three jets with high transverse momentum (p_T), one of which contains a b -hadron and is labelled as a b -tagged jet, j_B . In contrast to the dilepton analyses, the event signature contains only one neutrino, which originates from the leptonic W -boson decay. Hence, both the W -boson and the top-quark kinematics can be reconstructed and used to separate the signal from background. The main backgrounds are W + jets and $t\bar{t}$ events, where the latter background poses a major challenge in this measurement because of its similar kinematics and a ten times larger cross-section compared to the tW signal. An artificial neural network is trained to separate the signal from the $t\bar{t}$ background. The cross-section is extracted using a binned profile maximum-likelihood fit to a two-dimensional discriminant. This measurement, performed with tW single-lepton events, constitutes a cross-check of the previous results published in the dilepton channel.

2 ATLAS detector

The ATLAS experiment [13] at the LHC is a multipurpose particle detector with a forward–backward symmetric cylindrical geometry and a near 4π coverage in solid angle.¹ It consists of an inner tracking detector (ID) surrounded

¹ ATLAS uses a right-handed coordinate system with its origin at the nominal interaction point (IP) in the centre of the detector and the z -axis along the beam pipe. The x -axis points from the IP to the centre of the LHC ring, and the y -axis points upwards. Cylindrical coordinates

by a thin superconducting solenoid providing a 2 T axial magnetic field, electromagnetic and hadron calorimeters, and a muon spectrometer (MS). The ID provides charged-particle tracking in the pseudorapidity range $|\eta| < 2.5$. It consists of silicon pixel, silicon microstrip, and transition-radiation tracking detectors. Lead/liquid-argon (LAr) sampling calorimeters provide electromagnetic (EM) energy measurements with high granularity. An iron/scintillator-tile hadron calorimeter covers the central pseudorapidity range ($|\eta| < 1.7$). The endcap ($1.5 < |\eta| < 3.2$) and forward ($3.1 < |\eta| < 4.9$) regions are instrumented with LAr calorimeters for measurements of both EM and hadronic energy. The MS surrounds the calorimeters and includes a system of precision tracking chambers ($|\eta| < 2.7$) and fast detectors for triggering ($|\eta| < 2.4$). The magnet system for the MS consists of three large air-core toroidal magnets with eight superconducting coils. The field integral of the toroids ranges between 2.0 and 6.0 T m across most of the detector. Collisions producing interesting events are selected for storage with the trigger system [14]. For the data taken at $\sqrt{s} = 8$ TeV, a three-level trigger system was used to select events. The first-level trigger is implemented in hardware and uses a subset of the detector information. It reduced the accepted rate to at most 75 kHz. This was followed by two software-based trigger levels that together reduced the accepted event rate to 400 Hz on average, depending on the data-taking conditions.

3 Data and simulated event samples

The data considered in this analysis are from pp collisions at $\sqrt{s} = 8$ TeV and were taken with stable LHC beams and

Footnote 1 continued

(r, ϕ) are used in the transverse plane, ϕ being the azimuthal angle around the z -axis. The pseudorapidity is defined in terms of the polar angle θ as $\eta = -\ln \tan(\theta/2)$. Angular distance is measured in units of $\Delta R \equiv \sqrt{(\Delta\eta)^2 + (\Delta\phi)^2}$.

the ATLAS detector fully operational, corresponding to an integrated luminosity of 20.2 fb^{-1} .

Monte Carlo (MC) samples were produced using the full ATLAS detector simulation [15] implemented in GEANT 4 [16]. In addition, alternative MC samples, used to train the neural network and evaluate systematic uncertainties, were produced using ATLF2 [15], which provides a faster calorimeter simulation making use of parameterised showers to compute the energy deposited by the particles. Pile-up (additional pp interactions in the same or nearby bunch crossing) was modelled by overlaying simulated minimum-bias events generated with PYTHIA 8 [17]. Weights were assigned to the simulated events, such that the distribution of the number of pp interactions per bunch crossing in the simulation matches the corresponding distribution in the data, which has an average of 21 [18].

The tW signal events were simulated using the next-to-leading order (NLO) POWHEG method [19–21] implemented in the POWHEG BOX (v.1.0) generator (revision 2192) [22] with the CT10 parton distribution function (PDF) set [23] in the matrix-element calculation. The mass and width of the top-quark were set to $m_t = 172.5 \text{ GeV}$ and $\Gamma_t = 1.32 \text{ GeV}$, respectively. The top quark was assumed to decay exclusively into Wb . The parton shower, hadronisation and underlying event were simulated using PYTHIA 6 (v6.426) [24] with the LO CTEQ6L1 PDF set [25] and a corresponding set of tuned parameters called the Perugia 2011 (P2011C) tune [26]. The factorisation scale, μ_f , and renormalisation scale, μ_r , were set to m_t . Calculations involving tW production beyond LO included quantum interference with $t\bar{t}$ production. Double-counting of the contributions was avoided by using either the diagram-removal (DR) or the diagram-subtraction (DS) scheme [27, 28]. In the DR scheme, diagrams with a second on-shell top-quark propagator are removed from the amplitude, while in the DS scheme, a subtraction term cancels out the $t\bar{t}$ contribution to the cross-section when the top-quark propagator becomes on shell. Nominal MC samples were generated using the DR scheme. For the evaluation of systematic uncertainties, alternative samples were generated using the DS scheme, or using POWHEG BOX or MC@NLO (v4.06) [29], each interfaced with HERWIG (v6.520) [30]. For the HERWIG samples, the AUET2 tune [31] with the CT10 PDF was used and the underlying event was generated with JIMMY (v4.31) [32]. In addition, PYTHIA 6 (v6.427) samples with variations of μ_r and μ_f and the radiation tunes were used. The SM tW cross-section prediction at NLO including next-to-next-to-leading-log (NNLL) soft gluon corrections [33, 34] was calculated as $\sigma_{tW}^{\text{th}}(8 \text{ TeV}) = 22.4 \pm 0.6 (\text{scale}) \pm 1.4 (\text{PDF}) \text{ pb}$ assuming a top-quark mass, m_t , of 172.5 GeV . The first uncertainty accounts for renormalisation and factorisation scale variations (from $m_t/2$ to $2m_t$) and the second term covers the uncertainty in the parton distribution functions, evalu-

ated using the MSTW2008 PDF set [35] at next-to-next-to-leading order (NNLO).

The $t\bar{t}$ sample was generated with POWHEG BOX (v1.1) interfaced with PYTHIA 6 (v6.427) [36]. In the POWHEG BOX event generator, the CT10 PDFs were used, while the CTEQ6L1 PDFs were used for PYTHIA. The h_{damp} parameter, which effectively regulates the high- p_T gluon radiation, was set to m_t . The predicted $t\bar{t}$ production cross-section, $\sigma_{t\bar{t}}(8 \text{ TeV}) = 252.9_{-8.6}^{+6.4} (\text{scale}) \pm 11.7 (\text{PDF} + \alpha_s) \text{ pb}$, was calculated with the Top++2.0 program to NNLO in perturbative QCD, including soft-gluon resummation to NNLL [37]. The first uncertainty comes from the sum in quadrature of the effects of independently varying μ_r and μ_f . The uncertainty associated with variations in the PDFs and strong coupling constant, α_s , was evaluated following the PDF4LHC NLO prescription [38, 39], which defines the central value as the midpoint of the uncertainty envelope of three PDF sets: MSTW2008 NNLO [35], CT10 NNLO [40] and NNPDF2.3 5f FFN [41]. The same procedures as for the tW samples were employed to determine the uncertainties due to the NLO matching method and the parton shower and hadronisation. Samples to evaluate the scale uncertainties were produced in a similar way, varying μ_r and μ_f together with the Perugia tune, but also adding variations in the h_{damp} parameter (for the up-variation, h_{damp} was changed to $2m_t$, while for the down variation it was kept at m_t).

The other single-top-quark production processes, s -channel and t -channel, were also generated with POWHEG BOX (v1.1) coupled to PYTHIA 6 (v6.426), using the same PDF sets as described for the other top-quark processes above. The predicted cross-sections at $\sqrt{s} = 8 \text{ TeV}$ were calculated at NLO plus NNLL as $5.6 \pm 0.2 \text{ pb}$ for the s -channel [42, 43], and $87.8_{-1.9}^{+3.4} \text{ pb}$ for the t -channel [44, 45] process.

The multi-leg LO generator SHERPA (v1.4.1) [46–48], together with the CT10 PDF sets, was used to simulate vector-boson production in association with jets. SHERPA was used to generate the hard process as well as the parton shower and the modelling of the underlying event. Double-counting between the inclusive $V + n$ parton samples (with $V = W$ or Z) and samples with associated heavy-quark pair production was avoided consistently by using massive c - and b -quarks in the shower. The predicted NNLO W +jets cross-section with W decaying leptonically was calculated as $\sigma(pp \rightarrow \ell^\pm \nu_\ell X) = 36.3 \pm 1.9 \text{ nb}$ [49].² For Z + jets the cross-section was calculated at NNLO in QCD for leptonic Z decays as $\sigma(pp \rightarrow \ell^+ \ell^- X) = 3.72 \pm 0.19 \text{ nb}$ [49]. The ATLF2 simulation was used to generate these samples with sufficient statistics. For cross-checks of the W + jets modelling, an alternative sample generated with ALPGEN (v2.14) [50] with up to five additional partons, PYTHIA 6 (v6.426) and the CTEQ6L1 PDFs were used. Dibo-

² The quoted cross-section is the sum of decays into e , μ and τ .

son samples ($WW/WZ/ZZ$ + jets) were generated with HERWIG (v6.520) at LO QCD using the CTEQ6L1 PDF. The theoretical NLO cross-section for events with one lepton is 29.4 ± 1.5 pb [51].

Multijet events are selected in the analysis when they contain jets or photons misidentified as leptons or contain non-prompt leptons from hadron decays (both referred to as a ‘fake’ lepton). This background was estimated directly from data using the matrix method [52], which exploits differences in lepton identification and isolation properties between prompt and fake leptons. The data were processed with a second, ‘loose’ set of lepton selection criteria. The resulting sample was then corrected for efficiency differences between the two sets of cuts, and the contamination from events containing prompt leptons was subtracted. The efficiencies, lepton selection criteria, and uncertainties applied in this analysis are the same as in Ref. [52].

4 Object definitions

Primary vertex (PV) candidates in the interaction region are reconstructed from at least five tracks that satisfy a transverse momentum (p_T) of $p_T > 400$ MeV. The candidate with the highest sum of p_T^2 over all associated tracks is chosen as the hard-collision PV [53].

Muon candidates are reconstructed by matching segments or tracks in the MS with tracks found in the ID [54]. The candidates must have $p_T > 25$ GeV and be in the pseudorapidity range $|\eta| < 2.5$. The longitudinal impact parameter of the track relative to the hard-collision PV, $|z_{\text{vtx}}|$, is required to be smaller than 2 mm. In order to reject non-prompt muons, an isolation criterion is applied. The isolation variable is defined as the scalar sum of the transverse momenta of all tracks with $p_T > 1$ GeV (excluding the muon track) within a cone of size $\Delta R = 10 \text{ GeV}/p_T(\mu)$ around the muon’s direction. It is required to be less than 5% of the muon p_T . The selection efficiency after this requirement is measured to be about 97% in $Z \rightarrow \mu^+ \mu^-$ events.

Electron candidates are reconstructed from energy deposits (clusters) in the EM calorimeter, which match a well-reconstructed track in the ID [55]. Requirements on the transverse and longitudinal impact parameter of $|d_{\text{vtx}}| < 1$ mm and $|z_{\text{vtx}}| < 2$ mm, respectively, are applied. Electron candidates must have energy in the transverse plane $E_T > 25$ GeV and $|\eta_{\text{cluster}}| < 2.47$, where η_{cluster} denotes the pseudorapidity of the cluster. Clusters in the calorimeter barrel–endcap transition region, $1.37 < |\eta| < 1.52$, are excluded. An isolation requirement based on the deposited transverse energy in a cone of size $\Delta R = 0.2$ around the direction of the electron and the p_T sum of the tracks in a cone with $\Delta R = 0.3$ around the same direction is applied. This requirement is chosen to give a nearly uniform selection efficiency of 85% in p_T and

η , as measured in $Z \rightarrow e^+ e^-$ events. Electron candidates that share the ID track with a reconstructed muon candidate are vetoed.

Jets are reconstructed using the anti- k_r algorithm [56,57] with a radius parameter of $R = 0.4$ using topological clusters [58], calibrated with the Local Cluster Weighting method [59], as input to the jet finding. The jet energy is further corrected by subtracting the contribution from pile-up events and applying an MC-based and a data-based calibration. The jet vertex fraction (JVF) [60] variable is used to identify the primary vertex from which the jet originated. The JVF criterion suppresses pile-up jets with $p_T < 50$ GeV and $|\eta| < 2.4$. To avoid possible overlap between jets and electrons, jets that are closer than $\Delta R = 0.2$ to an electron are removed. Afterwards, remaining electron candidates overlapping with jets within a distance of $\Delta R = 0.4$ are rejected. Finally, muons overlapping with jets within $\Delta R = 0.4$ are removed.

The identification of jets originating from the hadronisation of a b -quark (b -tagging) is based on various algorithms exploiting the long lifetime, high mass and high decay multiplicity of b -hadrons as well as the properties of the b -quark fragmentation. The outputs of these algorithms are combined in a neural network classifier to maximise the b -tagging performance [61]. The choice of b -tagging working point represents a trade-off between the efficiency for identifying b -jets and rejection of other jets. The chosen working point for this analysis corresponds to a b -tagging efficiency of 70%. The corresponding c -quark-jet rejection factor is about 5 and the light-quark-jet rejection factor is about 120. These efficiencies and rejection factors were obtained using simulated $t\bar{t}$ events. The tagging efficiencies in the simulation are corrected to match the efficiencies measured in data [61].

The p_T^{miss} of the event, defined as the momentum imbalance in the plane transverse to the beam axis, is primarily due to neutrinos that escape detection. It is calculated as the negative vector sum of the transverse momenta of the reconstructed electrons, muons, jets and the clusters that are not associated with any of the previous objects (the ‘soft term’) [62]. Its magnitude is denoted E_T^{miss} .

5 Event selection

Events are required to have a hard-collision primary vertex. They also have to pass a single-lepton trigger requirement [14,63] and contain at least one electron or muon candidate with $p_T > 30$ GeV matched to the lepton that fired the trigger. The electron trigger requires an electron candidate, formed by an EM calorimeter cluster matched with a track, either with $E_T > 60$ GeV or with $E_T > 24$ GeV and additional isolation requirements. The muon trigger requires a muon candidate, defined as a reconstructed track in the muon spectrometer, either with $p_T > 36$ GeV or with $p_T > 24$ GeV

and isolation requirements. If there is another lepton candidate with a transverse momentum above 25 GeV, the event is rejected. This lepton veto guarantees orthogonality with respect to the dilepton analysis. The contribution from leptonically decaying τ -leptons is included. In the following, the electron or muon candidate is referred to as the lepton.

Events identified as containing jets from cosmic rays or beam-induced backgrounds or due to noise hot spots in the calorimeter are removed. Only jets with $p_T > 30$ GeV and $|\eta| < 2.4$ are considered in the analysis. Additionally, a requirement of $E_T^{\text{miss}} > 30$ GeV is applied, and the transverse mass³ of the leptonically decaying W boson must satisfy $m_T(W_L) > 50$ GeV.

In order to perform the measurement and validate the result, selected events are divided into different categories based on the jet and b -tagged jet multiplicities. The region with three jets of which one is b -tagged (3j1b) is called the signal region and is used to extract the tW cross-section. The region with four jets, two of them b -tagged (4j2b), contains a very pure sample of $t\bar{t}$ events and is used as the $t\bar{t}$ validation region to check the modelling of this background. Table 1 shows the expected and the observed numbers of events in the signal region after the event selection. All backgrounds except fake leptons, which is estimated using data-driven methods, are normalised to their expected cross-sections. The tW events constitute about 5% of the total number of events. The major backgrounds are $t\bar{t}$ production with about 58%, and W +jets production with about 28% of the total number of events. The W +jets events are subdivided into heavy flavour (HF), where a W boson is produced in association with b - or c -jets, and light flavour (LF). The total numbers of expected events agree within a few percent with the observed numbers of events.

6 Separation of signal from background

Differences between signal and background event kinematics are exploited to better separate them. The $t\bar{t}$ background is inherently difficult to distinguish from the signal, motivating the use of an artificial neural network (NN) implemented in the NeuroBayes framework [64, 65]. Detailed information about how the NN is used in single-top-quark analyses can be found in Ref. [66]. The NN input variables are selected such that they contribute significantly to the statistical separation power between signal and background, while avoiding variables that would lead to an increase of the expected uncertainty in the signal cross-section. The observable $m(W_H)$ (Fig. 2) provides very good separation of the signal from

Table 1 Expected signal and background and observed number of events in the signal 3j1b region. The cross-section for tW production is taken to be the theory prediction. The uncertainties include statistical and systematic uncertainties

Process	Signal region (3j1b)
tW ($\sigma_{tW}^{\text{th}} = 22.4$ pb)	6300 ± 600
$t\bar{t}$	77000 ± 6000
t , t -channel	4180 ± 290
t , s -channel	307 ± 19
W +jets, HF	31000 ± 14000
W +jets, LF	6000 ± 3000
Z +jets	3900 ± 1700
$WW/WZ/ZZ$ +jets	650 ± 280
Fake leptons	4300 ± 1900
Total background	128000 ± 18000
Total signal + background	134000 ± 18000
Observed	134633

the background, but is strongly affected by uncertainties in the reconstructed jet energies as well as uncertainties in the b -tagging in $t\bar{t}$ events. For this reason, $m(W_H)$ is not used in the NN; instead a two-dimensional discriminant is constructed from $m(W_H)$ and the response of the NN. The two-dimensional discriminant, explained in the following sections, allows the nuisance parameters affecting the variable $m(W_H)$ to be partially constrained.

6.1 Invariant mass of the hadronically decaying W boson

The variable $m(W_H)$ is computed from the four-momenta of the two selected untagged jets. For the signal and the $t\bar{t}$ background, the distribution of $m(W_H)$ exhibits a peak near the mass of the W boson, shown in Fig. 2a. The peak results from events where the two untagged jets are correctly matched to the hadronically decaying W boson. This is less likely to happen for $t\bar{t}$ events than for tW events due to the higher b -jet multiplicity and the limited b -tagging efficiency. On the other hand, the W +jets background does not feature such a peak since the W boson must decay leptonically for the events to pass the selection. Figure 2b shows the pre-fit distribution of $m(W_H)$, and also demonstrates good pre-fit modelling of the data.

6.2 Neural network

The NN is trained using simulated events with the two reconstructed untagged jets matched within $\Delta R < 0.35$ to the generator-level jets originating from a W -boson decay in the MC simulation and having a reconstructed mass of $65 \text{ GeV} < m(W_H) < 92.5 \text{ GeV}$. As events are required to

³ The transverse mass is calculated using the momentum of the lepton associated with the W boson, p_T^{miss} and the azimuthal angle between the two: $m_T(W_L) = m_T(\ell\nu) = \sqrt{2p_T(\ell) \cdot E_T^{\text{miss}} [1 - \cos(\Delta\phi(\ell, p_T^{\text{miss}}))]}$.

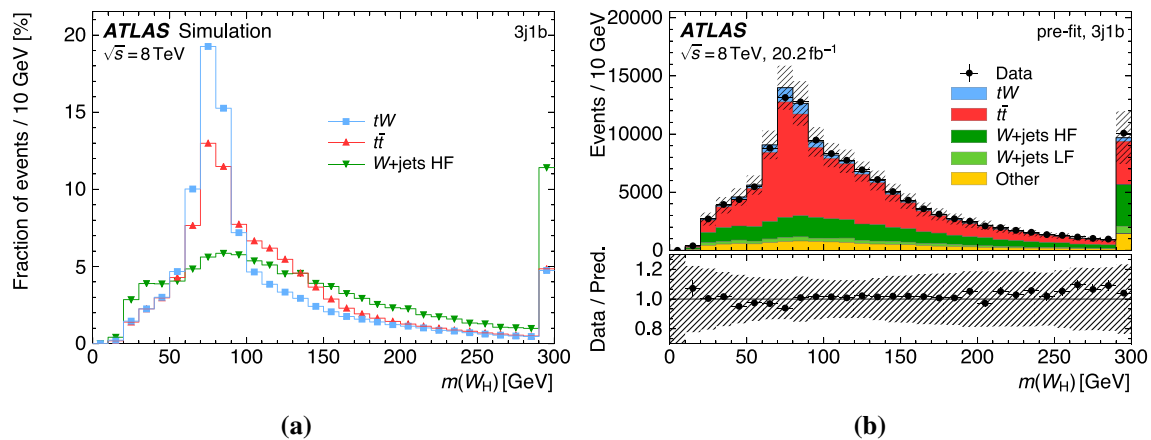


Fig. 2 **a** Shape of the reconstructed $m(W_H)$ distribution for signal and most important backgrounds in the signal (3j1b) region. The distribution for each process normalised to unity is shown. **b** Pre-fit $m(W_H)$ distribution in the 3j1b region. Small backgrounds are subsumed under ‘Other’. The simulated distributions are normalised to their theoretical

contain a lepton, only tW , $t\bar{t}$ and diboson events can have a pair of jets matched to the hadronic W -boson decay. Given that the contribution from diboson production is very small, the background sample used for the training consists entirely of $t\bar{t}$ events. Following the training procedure mentioned before, the following four variables (ordered by significance) are selected as input for the NN:

- the transverse momentum of the tW system, $p_T(W_H W_L j_B)$, divided by the sum of the objects’ transverse momenta,

$$\rho_T(W_H, W_L, j_B) = \frac{p_T(W_H W_L j_B)}{p_T(W_H) + p_T(W_L) + p_T(j_B)},$$

where the four-momentum of W_L is the sum of the four-momenta of the electron or muon and the neutrino, and the four-momentum of the neutrino is determined using E_T^{miss} from the solution of a quadratic equation.⁴ The use of $\rho_T(W_H, W_L, j_B)$, instead of the transverse momentum of the tW system, decreases the background contribution in the signal-like region of the NN response and results in a gain of sensitivity;

- the invariant mass of the reconstructed tW system, $m(W_L W_H j_B)$;

⁴ There are two solutions if $m_T(\ell\nu) < m_W$ and no real-valued solutions if $m_T(\ell\nu) > m_W$. In the first case, the ambiguity is resolved by picking the solution with the smaller $|p_z(\nu)|$. The latter case occurs if the measured E_T^{miss} is too large, and is resolved by adjusting E_T^{miss} until a real-valued solution is found, under the constraint that the adjustment be minimal in the transverse plane.

cross-sections. The dashed uncertainty band includes statistical and systematic uncertainties. The lower panels show the ratio of the observed and the predicted number of events in each bin. The last bin includes the overflow events.

- the absolute value of the difference between the pseudorapidities of the lepton and the leading untagged jet in p_T , $|\Delta\eta(\ell, j_{L1})|$;
- the absolute value of the pseudorapidity of the lepton, $|\eta(\ell)|$.

Figure 3 compares the data with the prediction for the NN input variables. For all variables, the simulation provides a good description of the data.

The distribution of the NN response is subdivided into eight bins, with the edges placed approximately at the 12.5% quantiles of a 50:50 mixture of tW and $t\bar{t}$ events. Figure 4a shows the shape of the NN response for the tW and $t\bar{t}$ processes and Fig. 4b presents the comparison between data and Monte Carlo simulation.

6.3 Two-dimensional discriminant

For the two-dimensional discriminant, $m(W_H)$ is used on the abscissa and the NN response on the ordinate of the two-dimensional discriminant. Outside of the aforementioned $m(W_H)$ range from 65 to 92.5 GeV, the bins corresponding to different values of the NN response are merged, i.e. the NN response is ignored. The two-dimensional distribution is presented in Fig. 5.

The bins are then rearranged on a one-dimensional axis in column-major order. The resulting one-dimensional distribution is presented in Fig. 6, together with a comparison of the shapes. The first three bins and the last ten bins correspond directly to the bins of $m(W_H)$ below 65 GeV and above 92.5 GeV respectively. In between are four blocks of eight bins, corresponding to the NN output in slices of $m(W_H)$.

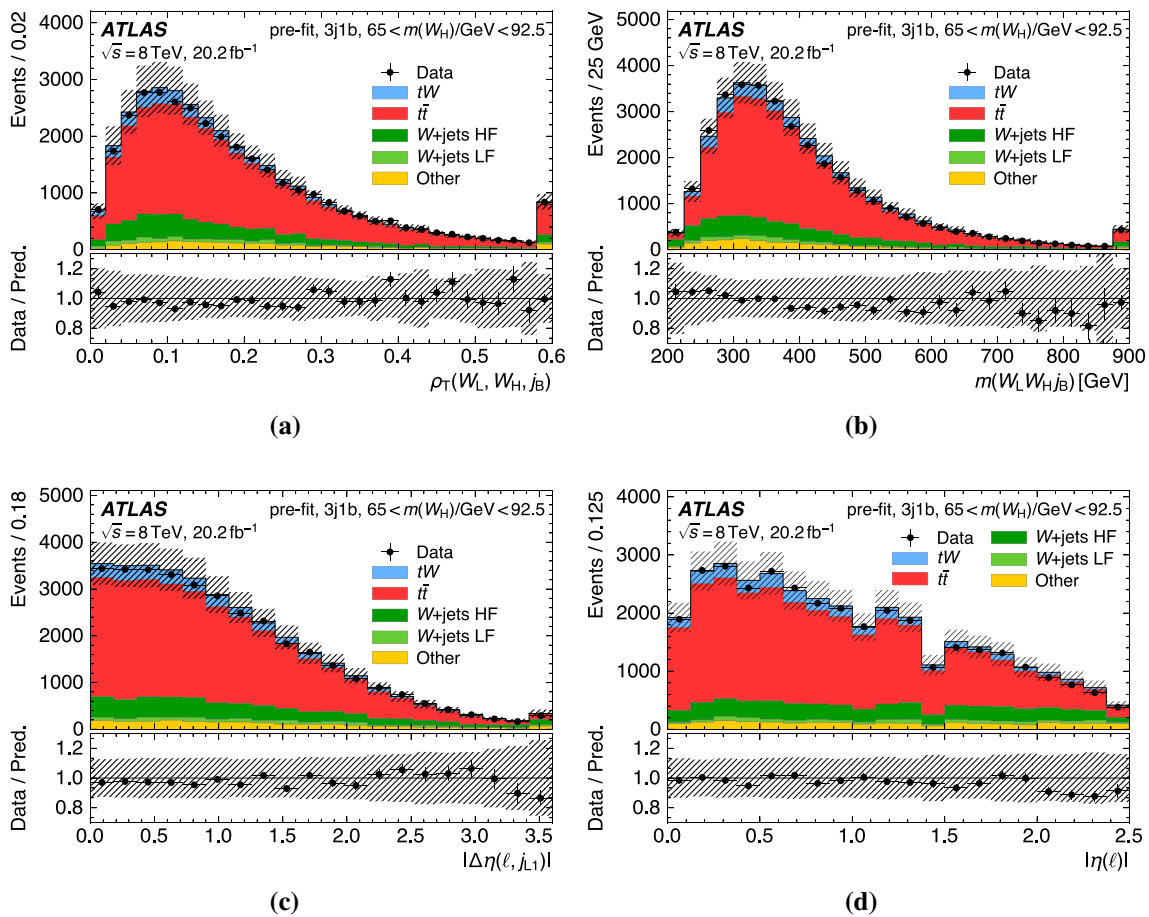


Fig. 3 Pre-fit distributions of the NN input variables in the tW signal (3j1b) region with $65 \text{ GeV} \leq m(W_H) \leq 92.5 \text{ GeV}$. Small backgrounds are subsumed under ‘Other’. The simulated distributions are normalised to their theoretical cross-sections. The dashed uncertainty band includes

statistical and systematic uncertainties. The last bin includes the overflow events. The lower panels show the ratio of the observed and the predicted number of events in each bin.

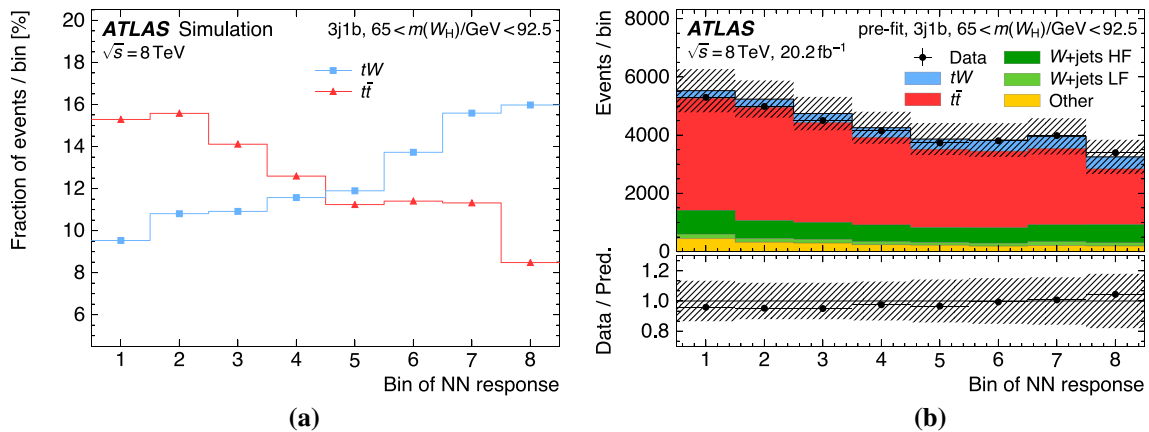


Fig. 4 a Shape of the NN response in the signal (3j1b) region. The distribution contains those events with $65 \text{ GeV} \leq m(W_H) \leq 92.5 \text{ GeV}$. The distributions for the tW process and the $t\bar{t}$ process normalised to unity are shown. **b** Pre-fit NN output distribution in the 3j1b region. Small backgrounds are subsumed under ‘Other’. The simulated distri-

butions are normalised to their theoretical cross-sections. The dashed uncertainty band includes statistical and systematic uncertainties. The lower panels show the ratio of the observed and the predicted number of events in each bin.

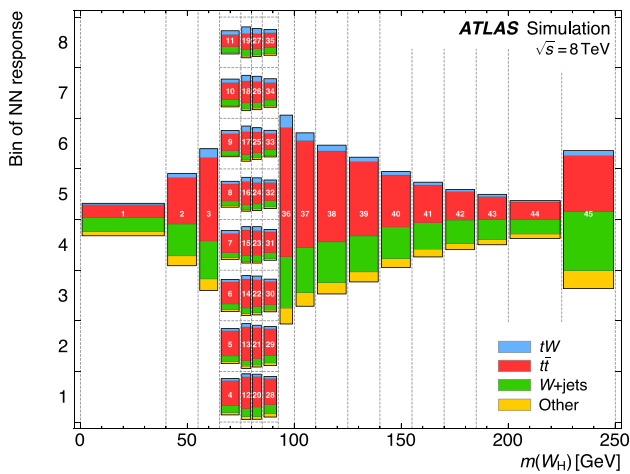


Fig. 5 Predicted distribution of the two-dimensional discriminant in the signal (3j1b) region. The proportions of the coloured areas reflect the expected composition in terms of tW , $t\bar{t}$, W +jets and other processes. The numbers correspond to the bin order when projecting the discriminant onto one axis as in Fig. 6. The last bin on the horizontal axis includes the overflow events

Inside each of the blocks, the tW -to- $t\bar{t}$ ratio increases significantly from left to right.

7 Systematic uncertainties

Uncertainties in the jet reconstruction arise from the jet energy scale (JES), jet energy resolution (JER), JVF requirement and jet reconstruction efficiency. The effect of the uncertainty in the JES [59] is evaluated by varying the reconstructed energies of the jets in the simulated samples. It is split into multiple components, taking into account the uncertainty in the calorimeter response, the detector simulation, the choice of MC event generator, the subtraction of pile-up, and differences in the detector response for jets initiated by a gluon, a light-flavour quark, or a b -quark. In a similar way, the JER uncertainty is represented using several components, which account for the uncertainty in different p_T and η regions of the detector, the difference between data and MC simulation, as well as the noise contribution in the forward detector region [59]. The uncertainty in jet reconstruction efficiency is estimated by randomly removing simulated jets from the events according to the jet reconstruction inefficiency measured with dijet events [67]. The JVF uncertainty is evaluated by varying the JVF criterion [60].

The scale factors used to correct the b -tagging efficiency in simulation compared to the efficiency in data are varied separately for b -jet, c -jet and light-flavour jets. Independent sources of uncertainty affecting the b -jet tagging efficiency and c -jet mis-tagging efficiency are considered depending on the jet kinematics, e.g. the variation of the b -quark jets is subdivided into 6 components. Uncertainties associated with the

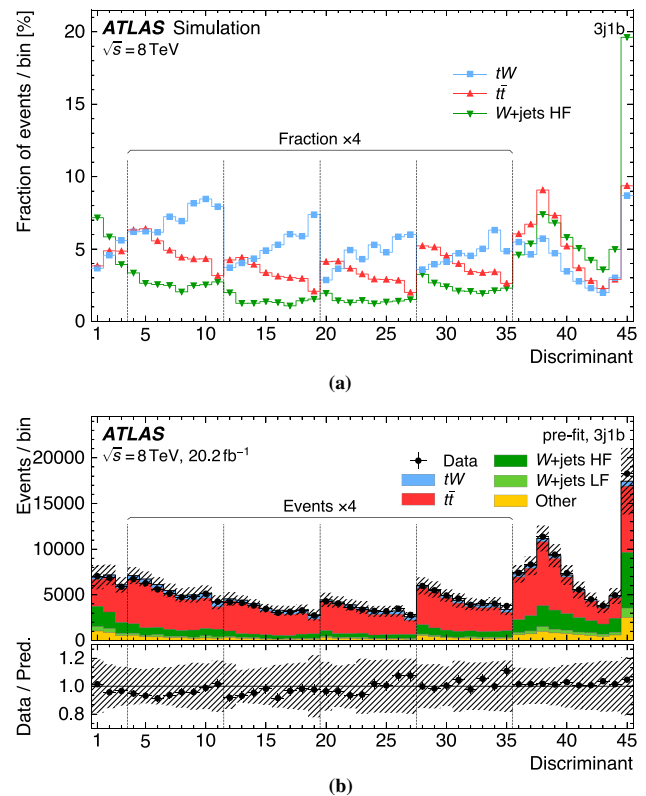


Fig. 6 **a** Shape distribution of the reconstructed discriminant in the tW signal (3j1b) region rearranged onto a one-dimensional distribution. The distribution for each process normalised to unity is shown. **b** Pre-fit distributions of the discriminant in the tW signal (3j1b) region. Small backgrounds are subsumed under ‘Other’. The simulated distributions are normalised to their theoretical cross-sections. The dashed uncertainty band includes statistical and systematic uncertainties. The lower panels show the ratio of the observed and the predicted number of events in each bin. The first three bins and the last ten bins correspond directly to (non-uniform) bins of $m(W_H)$. In between are four blocks of eight bins, corresponding to the NN output in slices of $m(W_H)$. Inside each of the blocks, the numbers of events are scaled by a factor of four for better visibility

lepton selection arise from the trigger, reconstruction, identification, isolation and lepton momentum scale and resolution [54,68,69].

All systematic uncertainties in the reconstruction of jets and leptons are propagated to the uncertainty in E_T^{miss} . In addition, dedicated uncertainties are assigned to the soft term of the E_T^{miss} , which accounts for energy deposits in the calorimeter which are not matched to high- p_T physics objects [62].

The uncertainty in the integrated luminosity for the data set used in this analysis is 1.9%. It is derived following the methodology detailed in Ref. [18]. This systematic uncertainty is applied to all contributions determined from the MC simulation.

Uncertainties stemming from theoretical models are evaluated using alternative MC samples for tW and $t\bar{t}$ processes.

The renormalisation and factorisation scales are varied in the matrix element and in the parton shower together with the amount of QCD radiation. Both scales are varied simultaneously in the matrix element and in the parton shower. The variation of both μ_r and μ_f by a factor of 0.5 is combined with the Perugia 2012radHi tune, while the variation of the scale parameters by a factor of 2.0 is combined with the Perugia 2012radLo tune [26]. This (radiation) uncertainty is considered uncorrelated between the tW and $t\bar{t}$ processes. The NLO matrix element generator uncertainty is estimated by comparing two NLO matching methods: POWHEG BOX and MC@NLO, both interfaced with HERWIG. The parton shower, hadronisation and underlying-event systematic uncertainties are computed by comparing POWHEG BOX with either PYTHIA or HERWIG. These are treated as fully correlated between the tW and $t\bar{t}$ processes. The uncertainty due to the treatment of the interference effects of the tW and $t\bar{t}$ processes is evaluated by using the tW DS scheme instead of the DR scheme, both generated using POWHEG BOX with PYTHIA. The effect of the PDF uncertainties on the acceptance is taken into account for both the tW signal and the $t\bar{t}$ background and treated as uncorrelated between the processes, following the studies in Ref. [70].

The uncertainties in the theoretical cross-section calculations are process dependent and vary from 4% for the t -channel to 6% for $t\bar{t}$ (see Sect. 3). In addition, there are large uncertainties in the Z/W +jets production cross-sections. For every jet an additional uncertainty of 24% is assumed [71]. The uncertainty in the normalisation of W/Z -boson production in association with three jets is 42%, and the rate of W -boson events with heavy-flavour jets is allowed to vary by an additional 20%.

The modelling of the W +jets background was cross-checked using ALPGEN with PYTHIA. The shape of the W +jets background was found to be consistent with the nominal SHERPA prediction. Hence no dedicated systematic uncertainty is assigned to the choice of generator, in order to avoid double-counting of the statistical uncertainty of the prediction (*model statistics*).

Uncertainties related to the modelling of the fake-lepton background take into account the choice of control region for the determination of the fake- and real-lepton efficiencies, the choice of parameterisation, and the normalisation of the prompt-lepton backgrounds in the determination of the efficiencies [52].

The uncertainty due to the limited size of the simulated samples and the fake-lepton background (*model statistics*) is estimated through the procedure detailed in Refs. [72, 73]: for every bin of the discriminant, an independent parameter is assigned which describes the variation of the predicted event rate constrained by its statistical uncertainty.

8 Statistical analysis

A binned profile maximum-likelihood fit to the discriminant in the signal region is used to determine the tW cross-section. The likelihood function is defined as a product of Poisson probability terms over all the bins of the discriminant in the signal region and Gaussian penalty terms,

$$L(\mu, \vec{\theta}; \vec{n}) = \prod_i^{\text{bins}} \text{Pois}(n_i; v_i(\mu, \vec{\theta})) \prod_k^{\text{NPs}} G(\theta_k; 0, 1),$$

where the n_i (v_i) is the observed (expected) number of events in each bin i of the discriminant. The expected number of events depends on the signal-strength parameter, μ , which is a multiplicative factor on the predicted signal cross-section. Nuisance parameters (NPs), θ_k , are used to encode the effects of the systematic uncertainties in the expected number of events. The Gaussian penalty terms model the external constraints on these parameters. The estimated parameters, denoted by $\hat{\mu}$ and $\hat{\theta}$, are obtained by maximising $L(\mu, \vec{\theta}; \vec{n})$.

The likelihood function is composed and evaluated with the HISTFACTORY program [74], part of the ROOSTATS framework [75]. The minimisation is performed with the MINUIT package [76], using MINOS to compute the error estimates.

The statistical significance, Z , of the result is estimated by comparing the likelihood values of two hypotheses. The background-only hypothesis is that there is no signal in the data (or equivalently, $\mu = 0$). The signal-plus-background hypothesis is that the signal exists with the signal strength obtained from the fit to data. With the asymptotic approximation [77], the significance is calculated using a test statistic based on the profile likelihood ratio,

$$Z^2 = -2 \log \frac{L(\mu = 0, \vec{\theta} = \hat{\theta}_{\mu=0})}{L(\mu = \hat{\mu}, \vec{\theta} = \hat{\theta})},$$

where $\hat{\theta}_{\mu=0}$ denotes the estimates of the nuisance parameters that maximise the likelihood function under the background-only hypothesis. The expected significance is calculated by replacing \vec{n} in the likelihood function with the Asimov dataset for the nominal signal-plus-background hypothesis ($\mu = 1, \vec{\theta} = \hat{\theta}$).

9 Cross-section measurement

The tW cross-section is extracted from the fit to data in the signal region. Given the Standard Model prediction, the extracted signal strength is expected to be $\hat{\mu} = 1.00 \pm 0.35$. The measured value is $\hat{\mu} = 1.16 \pm 0.31$, corresponding to an observed cross-section of $\sigma_{tW}^{\text{obs}} = 26 \pm 7$ pb, which is con-

Table 2 List of systematic uncertainties considered in the analysis and their relative impact on the observed signal strength, evaluated as described in the text. The ‘model statistics’ uncertainty is dominated by the W +jets background

Source	Uncertainty (%)
Jet energy scale	10
b -tagging	8
Jet energy resolution	7
E_T^{miss} reconstruction	7
Lepton reconstruction	4
Luminosity	3
Jet vertex fraction	3
$t\bar{t}$ radiation	10
tW radiation	9
tW – $t\bar{t}$ interference	7
$t\bar{t}$ cross-section normalisation	6
Other background cross-section normalisations	5
tW and $t\bar{t}$ parton shower	4
tW and $t\bar{t}$ NLO matching	3
PDF	1
Model statistics	11
Data statistics	4
Total	27

sistent with the Standard Model prediction. The observed (expected) significance is 4.5σ (3.9σ).

The (post-fit) impact of each systematic uncertainty on the measured signal strength is estimated by means of *conditional* fits, i.e. the fit is repeated while keeping the corresponding nuisance parameter fixed at the ± 1 standard deviation (sigma) value of the post-fit error interval. The resulting change in the estimate of the signal strength quantifies the impact of the uncertainty. For each nuisance parameter, the $+1$ and -1 sigma variations are found to be symmetric about the best-fit value to a very good approximation. Table 2 shows the impacts of the systematic uncertainties on the observed fit result, where the impacts of uncertainties with similar sources have been added in quadrature. The dominant uncertainties are due to the amount of QCD radiation in signal events and $t\bar{t}$ background, the JES and b -tagging, and the model statistics, including the limited size of the MC samples.

Some nuisance parameters are constrained by the data. For example, the normalisation uncertainty for W +jets events is reduced from 45% to 8%, because the assigned initial uncertainty is large and this background can be separated well from tW and $t\bar{t}$ events. By design of the discriminant, combinations of nuisance parameters that shift the peak in the $m(W_H)$ distribution are constrained, primarily the JES and choice of renormalisation scale together with the amount of

Table 3 Post-fit signal and background and observed number of events in the signal region and the $t\bar{t}$ validation region. The uncertainties include statistical plus all systematic uncertainties (cf. Sect. 7)

Process	Signal region (3j1b)	$t\bar{t}$ region (4j2b)
tW	7800 ± 1800	1300 ± 400
$t\bar{t}$	74500 ± 2100	36700 ± 2300
t , t -channel	4250 ± 200	590 ± 40
t , s -channel	315 ± 15	63 ± 4
W +jets, HF	34700 ± 3300	1400 ± 500
W +jets, other	5700 ± 1800	27 ± 19
Z +jets	3800 ± 1500	180 ± 90
$WW/WZ/ZZ$ +jets	640 ± 270	23 ± 13
Fake leptons	3000 ± 1600	5 ± 22
Total background	126900 ± 1900	38900 ± 2400
Total signal + background	134700 ± 500	40200 ± 2300
Observed	134633	41738

QCD radiation in signal and $t\bar{t}$ background. Also, the nuisance parameter for the NLO matching for tW and $t\bar{t}$ is constrained: the choice of MC@NLO is not supported by the data, reducing the impact of the choice from 9% pre-fit to 3% post-fit.

A few nuisance parameters are pulled away from the pre-fit expectation. For the parameter associated with the choice of parton-shower generator, a blend of PYTHIA and HERWIG gives the best description of the data, while the nominal PYTHIA prediction is disfavoured at the two-sigma level. The b -tagging parameter with the largest effect on the overall b -tagging efficiency is pulled by about one sigma, corresponding to a decrease of about 1% to 2% in the b -tagging efficiency compared to the pre-fit expectation. Given that the b -tagging calibration partially relies on dijet events [61], which correspond to a different environment regarding the production mechanism of the b -jets, the pull is reasonable.

Table 3 shows the post-fit event yields of each process. The uncertainties in the yields are computed taking the correlations between nuisance parameters and processes into account. The post-fit estimates are well within the uncertainties of the pre-fit expectation (Table 1), while most of their uncertainties are reduced. The normalisation uncertainty for W +HF jets changes from almost 50% to about 10%.

Figure 7 shows the post-fit distributions for the NN input variables, the NN output response and the $m(W_H)$ in the signal region. The post-fit plots use the parameter estimates obtained in the fit of the discriminant, including their uncertainties, and demonstrate a good description of the data.

Figure 8a shows that the data are well described by the model in the signal region. Figure 8b shows the strongest support for the validity of the fit result by comparing the

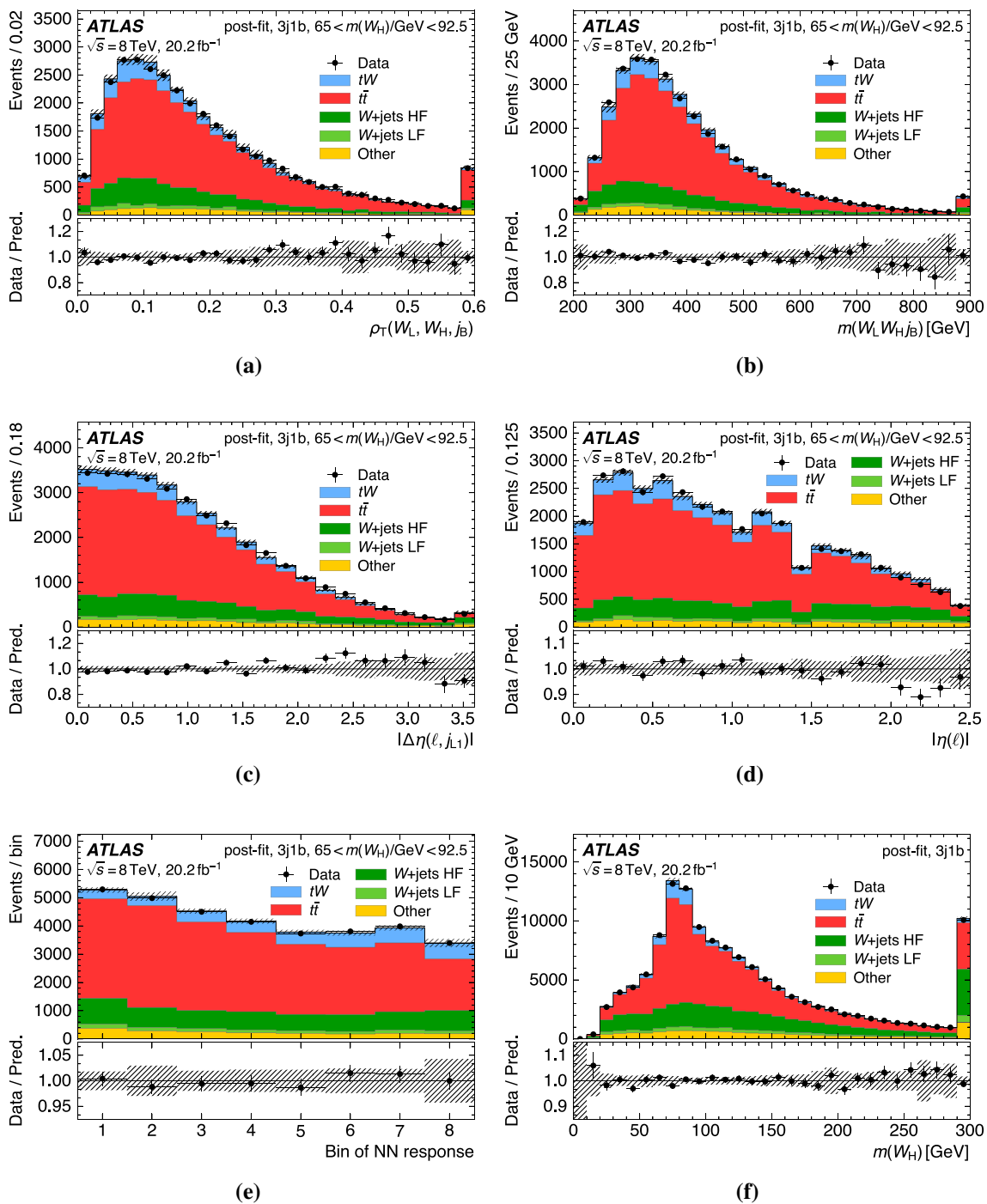


Fig. 7 **a–d** Post-fit distributions of the NN input variables, **e** NN discriminant and **f** $m(W_H)$ in the signal region. Small backgrounds are subsumed under ‘Other’. The dashed uncertainty band includes statis-

tical and systematic uncertainties. The last bin includes the overflow events, except for **e**. The lower panels show the ratio of the observed and the predicted number of events in each bin.

expected distributions and observed distributions in the $t\bar{t}$ validation region. It shows that the uncertainty due to the extrapolation from the signal region is small, and therefore provides a stringent test that the main background is well modelled.

10 Conclusion

The inclusive cross-section for the production of a single top quark in association with a W boson in the single-lepton channel is measured using an integrated luminosity

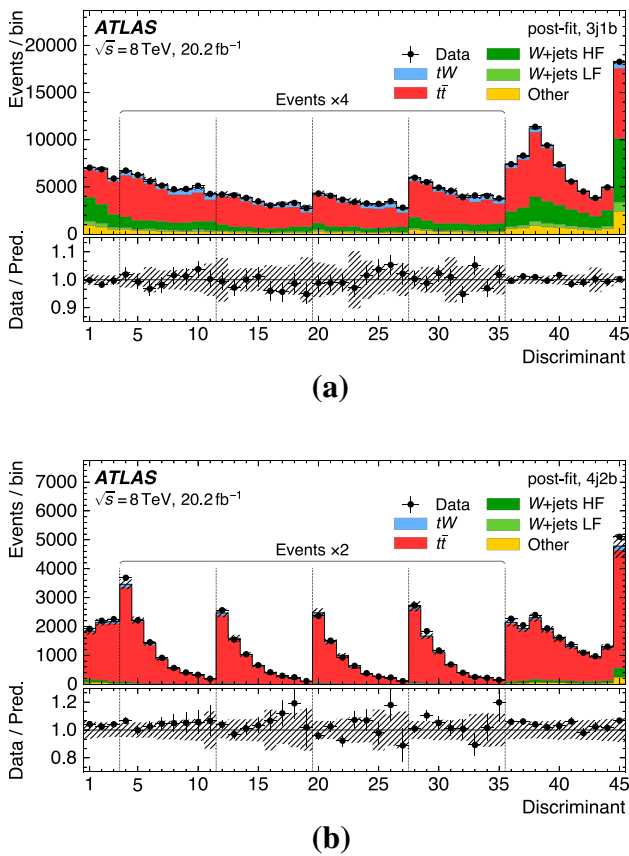


Fig. 8 Post-fit distributions of the discriminant in the **a** signal region and **b** validation region. Small backgrounds are subsumed under ‘Other’. The dashed uncertainty band includes statistical and systematic uncertainties. The lower panels show the ratio of the observed and the predicted number of events in each bin. The first three bins and the last ten bins correspond directly to (non-uniform) bins of $m(W_H)$. In between are four blocks of eight bins, corresponding to the NN output in slices of $m(W_H)$. Inside each of the blocks, the numbers of events are scaled by a factor of four (factor of two in 4j2b) for better visibility

of 20.2 fb^{-1} of $\sqrt{s} = 8 \text{ TeV}$ proton–proton collision data collected by the ATLAS detector at the LHC in 2012. A neural network is used to separate the signal from the $t\bar{t}$ background. A two-dimensional discriminant, built from the neural-network response and the mass of the hadronically decaying W boson, is used to extract the cross-section. Evidence for tW production in the single-lepton channel is obtained with an observed (expected) significance of 4.5 (3.9σ) standard deviations. The measured cross-section is:

$$\sigma_{tW}^{\text{meas.}} = 26 \pm 7 \text{ pb},$$

which is consistent with the SM expectation of $\sigma_{tW}^{\text{th.}} = 22.4 \pm 1.5 \text{ pb}$.

Acknowledgements We thank CERN for the very successful operation of the LHC, as well as the support staff from our institutions without whom ATLAS could not be operated efficiently. We acknowledge the support of ANPCyT, Argentina; YerPhI, Armenia; ARC, Australia; BMWFW and FWF, Austria; ANAS, Azerbaijan; SSTC,

Belarus; CNPq and FAPESP, Brazil; NSERC, NRC and CFI, Canada; CERN; ANID, Chile; CAS, MOST and NSFC, China; COLCIEN-CIAS, Colombia; MSMT CR, MPO CR and VSC CR, Czech Republic; DNRF and DNSRC, Denmark; IN2P3-CNRS and CEA-DRF/IRFU, France; SRNSFG, Georgia; BMBF, HGF and MPG, Germany; GSRT, Greece; RGC and Hong Kong SAR, China; ISF and Benozziyo Center, Israel; INFN, Italy; MEXT and JSPS, Japan; CNRST, Morocco; NWO, Netherlands; RCN, Norway; MNiSW and NCN, Poland; FCT, Portugal; MNE/IFA, Romania; JINR; MES of Russia and NRC KI, Russian Federation; MESTD, Serbia; MSSR, Slovakia; ARRS and MIZŠ, Slovenia; DST/NRF, South Africa; MICINN, Spain; SRC and Wallenberg Foundation, Sweden; SERI, SNSF and Cantons of Bern and Geneva, Switzerland; MOST, Taiwan; TAEK, Turkey; STFC, United Kingdom; DOE and NSF, USA. In addition, individual groups and members have received support from BCKDF, CANARIE, Compute Canada, CRC and IVADO, Canada; Beijing Municipal Science & Technology Commission, China; COST, ERC, ERDF, Horizon 2020 and Marie Skłodowska-Curie Actions, European Union; Investissements d’Avenir Labex, Investissements d’Avenir IDEX and ANR, France; DFG and AvH Foundation, Germany; Herakleitos, Thales and Aristeia programmes co-financed by EU-ESF and the Greek NSRF, Greece; BSF-NSF and GIF, Israel; La Caixa Banking Foundation, CERCA Programme Generalitat de Catalunya and PROMETEO and GenT Programmes Generalitat Valenciana, Spain; Göran Gustafssons Stiftelse, Sweden; The Royal Society and Leverhulme Trust, United Kingdom. The crucial computing support from all WLCG partners is acknowledged gratefully, in particular from CERN, the ATLAS Tier-1 facilities at TRIUMF (Canada), NDGF (Denmark, Norway, Sweden), CC-IN2P3 (France), KIT/GridKA (Germany), INFN-CNAF (Italy), NL-T1 (Netherlands), PIC (Spain), ASGC (Taiwan), RAL (UK) and BNL (USA), the Tier-2 facilities worldwide and large non-WLCG resource providers. Major contributors of computing resources are listed in Ref. [78].

Data Availability Statement This manuscript has no associated data or the data will not be deposited. [Authors’ comment: “All ATLAS scientific output is published in journals, and preliminary results are made available in Conference Notes. All are openly available, without restriction on use by external parties beyond copyright law and the standard conditions agreed by CERN. Data associated with journal publications are also made available: tables and data from plots (e.g. cross section values, likelihood profiles, selection efficiencies, cross section limits, ...) are stored in appropriate repositories such as HEPDATA (<http://hepdata.cedar.ac.uk/>). ATLAS also strives to make additional material related to the paper available that allows a reinterpretation of the data in the context of new theoretical models. For example, an extended encapsulation of the analysis is often provided for measurements in the framework of RIVET (<http://rivet.hepforge.org/>).” This information is taken from the ATLAS Data Access Policy, which is a public document that can be downloaded from <http://opendata.cern.ch/record/413> [opendata.cern.ch].]

Open Access This article is licensed under a Creative Commons Attribution 4.0 International License, which permits use, sharing, adaptation, distribution and reproduction in any medium or format, as long as you give appropriate credit to the original author(s) and the source, provide a link to the Creative Commons licence, and indicate if changes were made. The images or other third party material in this article are included in the article’s Creative Commons licence, unless indicated otherwise in a credit line to the material. If material is not included in the article’s Creative Commons licence and your intended use is not permitted by statutory regulation or exceeds the permitted use, you will need to obtain permission directly from the copyright holder. To view a copy of this licence, visit <http://creativecommons.org/licenses/by/4.0/>. Funded by SCOAP³.

References

1. T.M.P. Tait, C.-P. Yuan, Single top quark production as a window to physics beyond the standard model. *Phys. Rev. D* **63**, 014018 (2000). [arXiv:hep-ph/0007298](#)
2. Q.-H. Cao, J. Wudka, C.-P. Yuan, Search for new physics via single-top production at the LHC. *Phys. Lett. B* **658**, 50 (2007). [arXiv:0704.2809](#) [hep-ph]
3. ATLAS Collaboration, Search for B - L R-parity-violating top squarks in $\sqrt{s} = 13$ TeV pp collisions with the ATLAS experiment. *Phys. Rev. D* **97**, 032003 (2018). [arXiv:1710.05544](#) [hep-ex]
4. ATLAS Collaboration, Search for top-squark pair production in final states with one lepton, jets, and missing transverse momentum using 36 fb^{-1} of $\sqrt{s} = 13$ TeV pp collision data with the ATLAS detector. *JHEP* **06**, 108 (2018). [arXiv:1711.11520](#) [hep-ex]
5. ATLAS Collaboration, Evidence for the associated production of a W boson and a top quark in ATLAS at $\sqrt{s} = 7$ TeV. *Phys. Lett. B* **716**, 142 (2012). [arXiv:1205.5764](#) [hep-ex]
6. CMS Collaboration, Evidence for associated production of a single top quark and W boson in pp collisions at $\sqrt{s} = 7$ TeV. *Phys. Rev. Lett.* **110**, 022003 (2013). [arXiv:1209.3489](#) [hep-ex]
7. ATLAS Collaboration, Measurement of the production cross-section of a single top quark in association with a W boson at 8 TeV with the ATLAS experiment. *JHEP* **01**, 064 (2016). [arXiv:1510.03752](#) [hep-ex]
8. CMS Collaboration, Observation of the associated production of a single Top Quark and a W Boson in pp collisions at $\sqrt{s} = 8$ TeV. *Phys. Rev. Lett.* **112**, 231802 (2014). [arXiv:1401.2942](#) [hep-ex]
9. CMS Collaboration, Measurement of the production cross section for single top quarks in association with W bosons in proton-proton collisions at $\sqrt{s} = 13$ TeV. *JHEP* **10**, 117 (2018). [arXiv:1805.07399](#) [hep-ex]
10. ATLAS Collaboration, Measurement of the cross-section for producing a W boson in association with a single top quark in pp collisions at $\sqrt{s} = 13$ TeV with ATLAS. *JHEP* **01**, 063 (2018). [arXiv:1612.07231](#) [hep-ex]
11. ATLAS Collaboration, Measurement of differential cross-sections of a single top quark produced in association with a W boson at $\sqrt{s} = 13$ TeV with ATLAS. *Eur. Phys. J. C* **78**, 186 (2018). [arXiv:1712.01602](#) [hep-ex]
12. ATLAS Collaboration, Probing the quantum interference between singly and doubly resonant top-quark production in pp collisions at $\sqrt{s} = 13$ TeV with the ATLAS Detector. *Phys. Rev. Lett.* **121**, 152002 (2018). [arXiv:1806.04667](#) [hep-ex]
13. ATLAS Collaboration, The ATLAS experiment at the CERN large hadron collider. *JINST* **3**, S08003 (2008)
14. ATLAS Collaboration, Performance of the ATLAS Trigger System in. *Eur. Phys. J. C* **72**(2012), 1849 (2010). [arXiv:1110.1530](#) [hep-ex]
15. ATLAS Collaboration, The ATLAS Simulation Infrastructure. *Eur. Phys. J. C* **70**, 823 (2010). [arXiv:1005.4568](#) [physics.ins-det]
16. S. Agostinelli et al., GEANT4 – a simulation toolkit. *Nucl. Instrum. Methods A* **506**, 250 (2003)
17. T. Sjöstrand, S. Mrenna, P. Skands, A brief introduction to PYTHIA 8.1. *Comput. Phys. Commun.* **178**, 852 (2007). [arXiv:0710.3820](#) [hep-ph]
18. ATLAS Collaboration, Luminosity determination in pp collisions at $\sqrt{s} = 8$ TeV using the ATLAS detector at the LHC. *Eur. Phys. J. C* **76**, 653 (2016). [arXiv:1608.03953](#) [hep-ex]
19. P. Nason, A new method for combining NLO QCD with shower Monte Carlo algorithms. *JHEP* **11**, 040 (2004). [arXiv:hep-ph/0409146](#)
20. S. Frixione, P. Nason, C. Oleari, Matching NLO QCD computations with Parton shower simulations: the POWHEG method. *JHEP* **11**, 070 (2007). [arXiv:0709.2092](#) [hep-ph]
21. E. Re, Single-top Wt-channel production matched with Parton showers using the POWHEG method. *Eur. Phys. J. C* **71**, 1547 (2011). [arXiv:1009.2450](#) [hep-ph]
22. S. Alioli, P. Nason, C. Oleari, E. Re, A general framework for implementing NLO calculations in shower Monte Carlo programs: the POWHEG BOX. *JHEP* **06**, 1 (2010). [arXiv:1002.2581](#) [hep-ph]
23. H.-L. Lai et al., New Parton distributions for collider physics. *Phys. Rev. D* **82**, 074024 (2010). [arXiv:1007.2241](#) [hep-ph]
24. T. Sjöstrand, S. Mrenna, P. Skands, PYTHIA 6.4 physics and manual. *JHEP* **05**, 026 (2006). [arXiv:hep-ph/0603175](#)
25. P.M. Nadolsky et al., Implications of CTEQ global analysis for collider observables. *Phys. Rev. D* **78**, 013004 (2008). [arXiv:0802.0007](#) [hep-ph]
26. P.Z. Skands, Tuning Monte Carlo generators: the Perugia tunes. *Phys. Rev. D* **82**, 074018 (2010). [arXiv:1005.3457](#) [hep-ph]
27. S. Frixione, E. Laenen, P. Motylinski, B.R. Webber, C.D. White, Single-top hadroproduction in association with a W boson. *JHEP* **07**, 029 (2008). [arXiv:0805.3067](#) [hep-ph]
28. C.D. White, S. Frixione, E. Laenen, F. Maltoni, Isolating Wt production at the LHC. *JHEP* **11**, 074 (2009). [arXiv:0908.0631](#) [hep-ph]
29. S. Frixione, B.R. Webber, Matching NLO QCD computations and Parton shower simulations. *JHEP* **06**, 029 (2002). [arXiv:hep-ph/0204244](#)
30. G. Corcella et al., HERWIG 6: an event generator for hadron emission reactions with interfering gluons (including supersymmetric processes). *JHEP* **01**, 010 (2001). [arXiv:hep-ph/0011363](#)
31. ATLAS Collaboration, New ATLAS event generator tunes to 2010 data, ATL-PHYS-PUB-2011-008 (2011). <https://cds.cern.ch/record/1345343>
32. J.M. Butterworth, J.R. Forshaw, M.H. Seymour, Multiparton interactions in photoproduction at HERA. *Z. Für Phys. C* **72**, 637 (1996). [arXiv:hep-ph/9601371](#)
33. N. Kidonakis, Two-loop soft anomalous dimensions for single top quark associated production with a W^- or H^- . *Phys. Rev. D* **82**, 054018 (2010). [arXiv:1005.4451](#) [hep-ph]
34. N. Kidonakis, ‘Top Quark Production’, *Proceedings, Helmholtz International Summer School on Physics of Heavy Quarks and Hadrons (HQ 2013): JINR, Dubna, Russia, July 15-28, 2013* (2014), p. 139. [arXiv:1311.0283](#) [hep-ph]
35. A.D. Martin, W.J. Stirling, R.S. Thorne, G. Watt, Parton distributions for the LHC. *Eur. Phys. J. C* **63**, 189 (2009). [arXiv:0901.0002](#) [hep-ph] (ISSN: 1434-6052)
36. S. Frixione, P. Nason, G. Ridolfi, A positive-weight next-to-leading-order Monte Carlo for heavy flavour hadroproduction. *JHEP* **09**, 126 (2007). [arXiv:0707.3088](#) [hep-ph]
37. M. Czakon, A. Mitov, Top++: A program for the calculation of the top-pair cross-section at hadron colliders. *Comput. Phys. Commun.* **185**, 2930 (2014). [arXiv:1112.5675](#) [hep-ph]
38. M. Botje et al., The PDF4LHC Working Group Interim Recommendations (2011). <https://cds.cern.ch/record/1318947>
39. F. Demartin, S. Forte, E. Mariani, J. Rojo, A. Vicini, Impact of Parton distribution function and as uncertainties on Higgs boson production in gluon fusion at hadron colliders. *Phys. Rev. D* **82**, 014002 (2010). [arXiv:1004.0962](#) [hep-ph]
40. J. Gao et al., CT10 next-to-next-to-leading order global analysis of QCD. *Phys. Rev. D* **89**, 033009 (2014). [arXiv:1302.6246](#) [hep-ph]
41. NNPDF Collaboration, R.D. Ball et al., Parton distributions with LHC data. *Nucl. Phys. B* **867**, 244 (2013). [arXiv:1207.1303](#) [hep-ph]
42. N. Kidonakis, Next-to-next-to-leading logarithm resummation for s-channel single top quark production. *Phys. Rev. D* **81**, 054028 (2010). [arXiv:1001.5034](#) [hep-ph]
43. S. Alioli, P. Nason, C. Oleari, E. Re, NLO single-top production matched with shower in POWHEG: s- and t-channel contributions.

- JHEP **09**, 111 (2009). [arXiv:0907.4076](#) [hep-ph] [Erratum: JHEP **02** (2010) **011**]
44. N. Kidonakis, Next-to-next-to-leading-order collinear and soft gluon corrections for t-channel single top quark production. Phys. Rev. D **83**, 091503 (2011). [arXiv:1103.2792](#) [hep-ph]
 45. R. Frederix, E. Re, P. Torrielli, Single-top t-channel hadroproduction in the four-flavour scheme with POWHEG and aMC@NLO. JHEP **09**, 130 (2012). [arXiv:1207.5391](#) [hep-ph]
 46. T. Gleisberg et al., Event generation with SHERPA 1.1. JHEP **02**, 007 (2009). [arXiv:0811.4622](#) [hep-ph]
 47. S. Höche, F. Krauss, S. Schumann, F. Siegert, QCD matrix elements and truncated showers. JHEP **05**, 053 (2009). [arXiv:0903.1219](#) [hep-ph]
 48. S. Schumann, F. Krauss, A parton shower algorithm based on Catani-Seymour dipole factorisation. JHEP **03**, 038 (2008). [arXiv:0709.1027](#) [hep-ph]
 49. C. Anastasiou, L. Dixon, K. Melnikov, F. Petriello, High-precision QCD at hadron colliders: Electroweak gauge boson rapidity distributions at next-to-next-to leading order. Phys. Rev. D **69**, 094008 (2004). [arXiv:hep-ph/0312266](#)
 50. M.L. Mangano, M. Moretti, F. Piccinini, R. Pittau, A.D. Polosa, ALPGEN, a generator for hard multiparton processes in hadronic collisions. JHEP **07**, 001 (2003). [arXiv:hep-ph/0206293](#)
 51. J.M. Campbell, R. Ellis, An update on vector boson pair production at hadron colliders. Phys. Rev. D **60**, 113006 (1999). [arXiv:hep-ph/9905386](#)
 52. ATLAS Collaboration, Estimation of non-prompt and fake lepton backgrounds in final states with top quarks produced in proton-proton collisions at $\sqrt{s} = 8$ TeV with the ATLAS Detector, ATLAS-CONF-2014-058 (2014). <https://cds.cern.ch/record/1951336>
 53. ATLAS Collaboration, Reconstruction of primary vertices at the ATLAS experiment in Run 1 proton–proton collisions at the LHC. Eur. Phys. J. C **77**, 332 (2017). [arXiv:1611.10235](#) [hep-ex]
 54. ATLAS Collaboration, Measurement of the muon reconstruction performance of the ATLAS detector using 2011 and 2012 LHC proton–proton collision data. Eur. Phys. J. C **74**, 3130 (2014). [arXiv:1407.3935](#) [hep-ex]
 55. ATLAS Collaboration, Electron efficiency measurements with the ATLAS detector using , LHC proton-proton collision data. Eur. Phys. J. C **77**(2017), 195 (2012). [arXiv:1612.01456](#) [hep-ex]
 56. M. Cacciari, G.P. Salam, G. Soyez, The anti- k_r jet clustering algorithm. JHEP **04**, 063 (2008). [arXiv:0802.1189](#) [hep-ph]
 57. M. Cacciari, G.P. Salam, G. Soyez, FastJet user manual. Eur. Phys. J. C **72**, 1896 (2012). [arXiv:1111.6097](#) [hep-ph]
 58. ATLAS Collaboration, Topological cell clustering in the ATLAS calorimeters and its performance in LHC Run 1. Eur. Phys. J. C **77**, 490 (2017). [arXiv:1603.02934](#) [hep-ex]
 59. ATLAS Collaboration, Determination of jet calibration and energy resolution in proton-proton collisions at $\sqrt{s} = 8$ TeV using the ATLAS detector (2019). [arXiv:1910.04482](#) [hep-ex]
 60. ATLAS Collaboration, Performance of pile-up mitigation techniques for jets in pp collisions at $\sqrt{s} = 8$ TeV using the ATLAS detector. Eur. Phys. J. C **76**, 581 (2016). [arXiv:1510.03823](#) [hep-ex]
 61. ATLAS Collaboration, Performance of b-jet identification in the ATLAS experiment. JINST **11**, P04008 (2016). [arXiv:1512.01094](#) [hep-ex]
 62. ATLAS Collaboration, Performance of algorithms that reconstruct missing transverse momentum in $\sqrt{s} = 8$ TeV proton–proton collisions in the ATLAS detector. Eur. Phys. J. C **77**, 241 (2017). [arXiv:1609.09324](#) [hep-ex]
 63. ATLAS Collaboration, Performance of the ATLAS muon trigger in pp collisions at $\sqrt{s} = 8$ TeV. Eur. Phys. J. C **75**, 120 (2015). [arXiv:1408.3179](#) [hep-ex]
 64. M. Feindt, U. Kerzel, The NeuroBayes neural network package. Nucl. Instrum. Methods A **559**, 190 (2006)
 65. M. Feindt, A Neural Bayesian Estimator for Conditional Probability Densities (2004). [arXiv:physics/0402093](#) [physics.data-an]
 66. ATLAS Collaboration, Comprehensive measurements of t-channel single top-quark production cross sections at $\sqrt{s} = 7$ TeV with the ATLAS detector. Phys. Rev. D **90**, 112006 (2014). [arXiv:1406.7844](#) [hep-ex]
 67. ATLAS Collaboration, Jet energy measurement and its systematic uncertainty in proton-proton collisions at $\sqrt{s} = 7$ TeV with the ATLAS detector. Eur. Phys. J. C **75**, 17 (2015). [arXiv:1406.0076](#) [hep-ex]
 68. ATLAS Collaboration, Electron reconstruction and identification efficiency measurements with the ATLAS detector using the, LHC proton-proton collision data. Eur. Phys. J. C **74**(2014), 2941 (2011). [arXiv:1404.2240](#) [hep-ex]
 69. ATLAS Collaboration, Electron performance measurements with the ATLAS detector using the, LHC proton-proton collision data. Eur. Phys. J. C **72**(2012), 1909 (2010). [arXiv:1110.3174](#) [hep-ex]
 70. ATLAS Collaboration, Study of correlation of PDF uncertainty in single top and top pair production at the LHC. ATL-PHYS-PUB-2015-010 (2015). <https://cds.cern.ch/record/2020601>
 71. J. Alwall et al., Comparative study of various algorithms for the merging of parton showers and matrix elements in hadronic collisions. Eur. Phys. J. C **53**, 473 (2008). [arXiv:0706.2569](#) [hep-ph]
 72. R.J. Barlow, C. Beeston, Fitting using finite Monte Carlo samples. Comput. Phys. Commun. **77**, 219 (1993)
 73. J. Conway, Incorporating nuisance parameters in likelihoods for multisource spectra (2011). [arXiv:1103.0354](#) [physics.data-an]
 74. K. Cranmer, G. Lewis, L. Moneta, A. Shibata, W. Verkerke, HistFactory: A tool for creating statistical models for use with RooFit and RooStats (2012). <https://cds.cern.ch/record/1456844>
 75. L. Moneta, K. Belasco, K. S. Cranmer, S. Kreiss, A. Lazzaro et al., The RooStatsProject (2010). [arXiv:1009.1003](#) [physics.data-an]
 76. F. James, M. Roos, Minuit – a system for function minimization and analysis of the parameter errors and correlations. Comput. Phys. Commun. **10**, 343 (1975)
 77. G. Cowan, K. Cranmer, E. Gross, O. Vitells, Asymptotic formulae for likelihood-based tests of new physics. Eur. Phys. J. C **71**, 1554 (2011). [arXiv:1007.1727](#) [physics.data-an] [Erratum: Eur. Phys. J. C **73** (2013) **2501**]
 78. ATLAS Collaboration, ATLAS Computing Acknowledgements. ATL-SOFT-PUB-2020-001 (2020). <https://cds.cern.ch/record/2717821>

ATLAS Collaboration

G. Aad¹⁰², B. Abbott¹²⁹, D. C. Abbott¹⁰³, A. Abed Abud^{71a,71b}, K. Abeling⁵³, D. K. Abhayasinghe⁹⁴, S. H. Abidi¹⁶⁸, O. S. AbouZeid⁴⁰, N. L. Abraham¹⁵⁷, H. Abramowicz¹⁶², H. Abreu¹⁶¹, Y. Abulaiti⁶, B. S. Acharya^{67a,67b,o}, B. Achkar⁵³, S. Adachi¹⁶⁴, L. Adam¹⁰⁰, C. Adam Bourdarios⁵, L. Adamczyk^{84a}, L. Adamek¹⁶⁸, J. Adelman¹²¹, M. Adersberger¹¹⁴, A. Adiguzel^{12c.ak}, S. Adorni⁵⁴, T. Adye¹⁴⁴, A. A. Affolder¹⁴⁶, Y. Afik¹⁶¹, C. Agapopoulou⁶⁵, M. N. Agaras³⁸, A. Aggarwal¹¹⁹, C. Agheorghiesei^{27c}, J. A. Aguilar-Saavedra^{140f,140a.aj}, F. Ahmadov⁸⁰, W. S. Ahmed¹⁰⁴, X. Ai¹⁸, G. Aielli^{74a,74b}, S. Akatsuka⁸⁶, T. P. A. Åkesson⁹⁷, E. Akilli⁵⁴, A. V. Akimov¹¹¹, K. Al Khoury⁶⁵, G. L. Alberghi^{23b,23a}, J. Albert¹⁷⁷, M. J. Alconada Verzini¹⁶², S. Alderweireldt³⁶, M. Aleksa³⁶, I. N. Aleksandrov⁸⁰, C. Alexa^{27b}, D. Alexandre¹⁹, T. Alexopoulos¹⁰, A. Alfonsi¹²⁰, F. Alfonsi^{23b,23a}, M. Alhroob¹²⁹, B. Ali¹⁴², M. Aliev¹⁵⁶, G. Alimonti^{69a}, J. Alison³⁷, S. P. Alkire¹⁴⁹, C. Allaire⁶⁵, B. M. M. Allbrooke¹⁵⁷, B. W. Allen¹³², P. P. Allport²¹, A. Aloisio^{70a,70b}, A. Alonso⁴⁰, F. Alonso⁸⁹, C. Alpigiani¹⁴⁹, A. A. Alshehri⁵⁷, M. Alvarez Estevez⁹⁹, D. Álvarez Piqueras¹⁷⁵, M. G. Alvigi^{70a,70b}, Y. Amaral Coutinho^{81b}, A. Ambler¹⁰⁴, L. Ambroz¹³⁵, C. Amelung²⁶, D. Amidei¹⁰⁶, S. P. Amor Dos Santos^{140a}, S. Amoroso⁴⁶, C. S. Amrouche⁵⁴, F. An⁷⁹, C. Anastopoulos¹⁵⁰, N. Andari¹⁴⁵, T. Andeen¹¹, C. F. Anders^{61b}, J. K. Anders²⁰, A. Andreazza^{69a,69b}, V. Andrei^{61a}, C. R. Anelli¹⁷⁷, S. Angelidakis³⁸, A. Angerami³⁹, A. V. Anisenkov^{122b,122a}, A. Annovi^{72a}, C. Antel^{61a}, M. T. Anthony¹⁵⁰, E. Antipov¹³⁰, M. Antonelli⁵¹, D. J. A. Antrim¹⁷², F. Anulli^{73a}, M. Aoki⁸², J. A. Aparisi Pozo¹⁷⁵, L. Aperio Bella^{15a}, G. Arabidze¹⁰⁷, J. P. Araque^{140a}, V. Araujo Ferraz^{81b}, R. Araujo Pereira^{81b}, C. Arcangeletti⁵¹, A. T. H. Arce⁴⁹, F. A. Arduh⁸⁹, J.-F. Arguin¹¹⁰, S. Argyropoulos⁷⁸, J.-H. Arling⁴⁶, A. J. Armbruster³⁶, A. Armstrong¹⁷², O. Arnaez¹⁶⁸, H. Arnold¹²⁰, Z. P. Arrubarrena Tame¹¹⁴, G. Artoni¹³⁵, S. Artz¹⁰⁰, S. Asai¹⁶⁴, N. Asbah⁵⁹, E. M. Asimakopoulou¹⁷³, L. Asquith¹⁵⁷, J. Assahsah^{35d}, K. Assamagan²⁹, R. Astalos^{28a}, R. J. Atkin^{33a}, M. Atkinson¹⁷⁴, N. B. Atlay¹⁹, H. Atmani⁶⁵, K. Augsten¹⁴², G. Avolio³⁶, R. Avramidou^{60a}, M. K. Ayoub^{15a}, A. M. Azoulay^{169b}, G. Azuelos^{110.ax}, H. Bachacou¹⁴⁵, K. Bachas^{68a,68b}, M. Backes¹³⁵, F. Backman^{45a,45b}, P. Bagnaia^{73a,73b}, M. Bahmani⁸⁵, H. Bahrasemani¹⁵³, A. J. Bailey¹⁷⁵, V. R. Bailey¹⁷⁴, J. T. Baines¹⁴⁴, M. Bajic⁴⁰, C. Bakalis¹⁰, O. K. Baker¹⁸⁴, P. J. Bakker¹²⁰, D. Bakshi Gupta⁸, S. Balaji¹⁵⁸, E. M. Baldin^{122b,122a}, P. Balek¹⁸¹, F. Balli¹⁴⁵, W. K. Balunas¹³⁵, J. Balz¹⁰⁰, E. Banas⁸⁵, A. Bandyopadhyay²⁴, Sw. Banerjee^{182.j}, A. A. E. Bannoura¹⁸³, L. Barak¹⁶², W. M. Barbe³⁸, E. L. Barberio¹⁰⁵, D. Barberis^{55b,55a}, M. Barbero¹⁰², G. Barbour⁹⁵, T. Barillari¹¹⁵, M.-S. Barisits³⁶, J. Barkeloo¹³², T. Barklow¹⁵⁴, R. Barnea¹⁶¹, S. L. Barnes^{60c}, B. M. Barnett¹⁴⁴, R. M. Barnett¹⁸, Z. Barnovska-Blenessy^{60a}, A. Baroncelli^{60a}, G. Barone²⁹, A. J. Barr¹³⁵, L. Barranco Navarro^{45a,45b}, F. Barreiro⁹⁹, J. Barreiro Guimarães da Costa^{15a}, S. Barsov¹³⁸, R. Bartoldus¹⁵⁴, G. Bartolini¹⁰², A. E. Barton⁹⁰, P. Bartos^{28a}, A. Basalae⁴⁶, A. Bassalat^{65.ar}, M. J. Basso¹⁶⁸, R. L. Bates⁵⁷, S. Batlamous^{35e}, J. R. Batley³², B. Batool¹⁵², M. Battaglia¹⁴⁶, M. Bauc^{73a,73b}, F. Bauer¹⁴⁵, K. T. Bauer¹⁷², H. S. Bawa^{31.m}, J. B. Beacham⁴⁹, T. Beau¹³⁶, P. H. Beauchemin¹⁷¹, F. Becherer⁵², P. Bechtel²⁴, H. C. Beck⁵³, H. P. Beck^{20.s}, K. Becker⁵², M. Becker¹⁰⁰, C. Becot⁴⁶, A. Beddall^{12d}, A. J. Beddall^{12a}, V. A. Bednyakov⁸⁰, M. Bedognetti¹²⁰, C. P. Bee¹⁵⁶, T. A. Beermann¹⁸³, M. Begalli^{81b}, M. Begel²⁹, A. Behera¹⁵⁶, J. K. Behr⁴⁶, F. Beisiegel²⁴, A. S. Bell⁹⁵, G. Bella¹⁶², L. Bellagamba^{23b}, A. Bellerive³⁴, P. Bellos⁹, K. Beloborodov^{122b,122a}, K. Belotskiy¹¹², N. L. Belyaev¹¹², D. Benchekroun^{35a}, N. Benekos¹⁰, Y. Benhammou¹⁶², D. P. Benjamin⁶, M. Benoit⁵⁴, J. R. Bensinger²⁶, S. Bentvelsen¹²⁰, L. Beresford¹³⁵, M. Beretta⁵¹, D. Berge⁴⁶, E. Bergeas Kuutmann¹⁷³, N. Berger⁵, B. Bergmann¹⁴², L. J. Bergsten²⁶, J. Beringer¹⁸, S. Berlendis⁷, G. Bernardi¹³⁶, C. Bernius¹⁵⁴, F. U. Bernlochner²⁴, T. Berry⁹⁴, P. Berta¹⁰⁰, C. Bertella^{15a}, I. A. Bertram⁹⁰, O. Bessidskaia Bylund¹⁸³, N. Besson¹⁴⁵, A. Bethani¹⁰¹, S. Bethke¹¹⁵, A. Betti⁴², A. J. Bevan⁹³, J. Beyer¹¹⁵, D. S. Bhattacharya¹⁷⁸, P. Bhattarai²⁶, R. Bi¹³⁹, R. M. Bianchi¹³⁹, O. Biebel¹¹⁴, D. Biedermann¹⁹, R. Bielski³⁶, K. Bierwagen¹⁰⁰, N. V. Biesuz^{72a,72b}, M. Biglietti^{75a}, T. R. V. Billoud¹¹⁰, M. Bindi⁵³, A. Bingul^{12d}, C. Bini^{73a,73b}, S. Biondi^{23b,23a}, M. Birman¹⁸¹, T. Bisanz⁵³, J. P. Biswal¹⁶², D. Biswas^{182.j}, A. Bitadze¹⁰¹, C. Bittrich⁴⁸, K. Björke¹³⁴, K. M. Black²⁵, T. Blazek^{28a}, I. Bloch⁴⁶, C. Blocker²⁶, A. Blue⁵⁷, U. Blumenschein⁹³, G. J. Bobbink¹²⁰, V. S. Bobrovnikov^{122b,122a}, S. S. Bocchetta⁹⁷, A. Bocci⁴⁹, D. Bogavac¹⁴, A. G. Bogdanchikov^{122b,122a}, C. Bohm^{45a}, V. Boisvert⁹⁴, P. Bokan⁵³, T. Bold^{84a}, A. S. Boldyrev¹¹³, A. E. Bolz^{61b}, M. Bomben¹³⁶, M. Bona⁹³, J. S. Bonilla¹³², M. Boonekamp¹⁴⁵, C. D. Booth⁹⁴, H. M. Borecka-Bielska⁹¹, A. Borisov¹²³, G. Borissov⁹⁰, J. Bortfeldt³⁶, D. Bortoletto¹³⁵, D. Boscherini^{23b}, M. Bosman¹⁴, J. D. Bossio Sola¹⁰⁴, K. Bouaouda^{35a}, J. Boudreau¹³⁹, E. V. Bouhova-Thacker⁹⁰, D. Boumediene³⁸, S. K. Boutle⁵⁷, A. Boveia¹²⁷, J. Boyd³⁶, D. Boyle^{33c.as}, I. R. Boyko⁸⁰, A. J. Bozson⁹⁴, J. Bracinik²¹, N. Brahimi¹⁰², G. Brandt¹⁸³,

O. Brandt³², F. Braren⁴⁶, B. Brau¹⁰³, J. E. Brau¹³², W. D. Breaden Madden⁵⁷, K. Brendlinger⁴⁶, L. Brenner⁴⁶, R. Brenner¹⁷³, S. Bressler¹⁸¹, B. Brickwedde¹⁰⁰, D. L. Briglin²¹, D. Britton⁵⁷, D. Britzger¹¹⁵, I. Brock²⁴, R. Brock¹⁰⁷, G. Brooijmans³⁹, W. K. Brooks^{147d}, E. Brost¹²¹, J. H. Broughton²¹, P. A. Bruckman de Renstrom⁸⁵, D. Bruncko^{28b}, A. Bruni^{23b}, G. Bruni^{23b}, L. S. Bruni¹²⁰, S. Bruno^{74a,74b}, M. Bruschi^{23b}, N. Brusino¹³⁹, P. Bryant³⁷, L. Bryngemark⁹⁷, T. Buanes¹⁷, Q. Buat³⁶, P. Buchholz¹⁵², A. G. Buckley⁵⁷, I. A. Budagov⁸⁰, M. K. Bugge¹³⁴, F. Bühner⁵², O. Bulekov¹¹², T. J. Burch¹²¹, S. Burdin⁹¹, C. D. Burgard¹²⁰, A. M. Burger¹³⁰, B. Burghgrave⁸, J. T. P. Burr⁴⁶, C. D. Burton¹¹, J. C. Burzynski¹⁰³, V. Büscher¹⁰⁰, E. Buschmann⁵³, P. J. Bussey⁵⁷, J. M. Butler²⁵, C. M. Buttar⁵⁷, J. M. Butterworth⁹⁵, P. Butti³⁶, W. Buttinger³⁶, C. J. Buxo Vazquez¹⁰⁷, A. Buzatu¹⁵⁹, A. R. Buzykaev^{122b,122a}, G. Cabras^{23b,23a}, S. Cabrera Urbán¹⁷⁵, D. Caforio⁵⁶, H. Cai¹⁷⁴, V. M. M. Cairo¹⁵⁴, O. Cakir^{4a}, N. Calace³⁶, P. Calafiura¹⁸, A. Calandri¹⁰², G. Calderini¹³⁶, P. Calfayan⁶⁶, G. Callea⁵⁷, L. P. Caloba^{81b}, A. Caltabiano^{74a,74b}, S. Calvente Lopez⁹⁹, D. Calvet³⁸, S. Calvet³⁸, T. P. Calvet¹⁵⁶, M. Calvetti^{72a,72b}, R. Camacho Toro¹³⁶, S. Camarda³⁶, D. Camarero Munoz⁹⁹, P. Camarri^{74a,74b}, D. Cameron¹³⁴, R. Caminal Armadans¹⁰³, C. Camincher³⁶, S. Campana³⁶, M. Campanelli⁹⁵, A. Camplani⁴⁰, A. Campoverde¹⁵², V. Canale^{70a,70b}, A. Canesse¹⁰⁴, M. Cano Bret^{60c}, J. Cantero¹³⁰, T. Cao¹⁶², Y. Cao¹⁷⁴, M. D. M. Capeans Garrido³⁶, M. Capua^{41b,41a}, R. Cardarelli^{74a}, F. Cardillo¹⁵⁰, G. Carducci^{41b,41a}, I. Carli¹⁴³, T. Carli³⁶, G. Carlino^{70a}, B. T. Carlson¹³⁹, L. Carminati^{69a,69b}, R. M. D. Carney^{45a,45b}, S. Caron¹¹⁹, E. Carquin^{147d}, S. Carrá⁴⁶, J. W. S. Carter¹⁶⁸, M. P. Casado^{14.e}, A. F. Casha¹⁶⁸, D. W. Casper¹⁷², R. Castelijm¹²⁰, F. L. Castillo¹⁷⁵, V. Castillo Gimenez¹⁷⁵, N. F. Castro^{140a,140e}, A. Catinaccio³⁶, J. R. Catmore¹³⁴, A. Cattai³⁶, J. Caudron²⁴, V. Cavaliere²⁹, E. Cavallaro¹⁴, M. Cavalli-Sforza¹⁴, V. Cavasinni^{72a,72b}, E. Celebi^{12b}, F. Ceradini^{75a,75b}, L. Cerda Alberich¹⁷⁵, K. Cerny¹³¹, A. S. Cerqueira^{81a}, A. Cerri¹⁵⁷, L. Cerrito^{74a,74b}, F. Cerutti¹⁸, A. Cervelli^{23b,23a}, S. A. Cetin^{12b}, Z. Chadi^{35a}, D. Chakraborty¹²¹, S. K. Chan⁵⁹, W. S. Chan¹²⁰, W. Y. Chan⁹¹, J. D. Chapman³², B. Chargeishvili^{160b}, D. G. Charlton²¹, T. P. Charman⁹³, C. C. Chau³⁴, S. Che¹²⁷, S. Chekanov⁶, S. V. Chekulaev^{169a}, G. A. Chelkov^{80.ap}, M. A. Chelstowska³⁶, B. Chen⁷⁹, C. Chen^{60a}, C. H. Chen⁷⁹, H. Chen²⁹, J. Chen^{60a}, J. Chen³⁹, S. Chen¹³⁷, S. J. Chen^{15c}, X. Chen^{15b.aw}, Y. Chen⁸³, Y-H. Chen⁴⁶, H. C. Cheng^{63a}, H. J. Cheng^{15a}, A. Cheplakov⁸⁰, E. Cheremushkina¹²³, R. Cherkaoui El Moursli^{35c}, E. Cheu⁷, K. Cheung⁶⁴, T. J. A. Chevaléras¹⁴⁵, L. Chevalier¹⁴⁵, V. Chiarella⁵¹, G. Chiarelli^{72a}, G. Chiodini^{68a}, A. S. Chisholm²¹, A. Chitan^{27b}, I. Chiu¹⁶⁴, Y. H. Chiu¹⁷⁷, M. V. Chizhov⁸⁰, K. Choi⁶⁶, A. R. Chomont^{73a,73b}, S. Chouridou¹⁶³, Y. S. Chow¹²⁰, M. C. Chu^{63a}, X. Chu^{15a,15d}, J. Chudoba¹⁴¹, A. J. Chuinard¹⁰⁴, J. J. Chwastowski⁸⁵, L. Chytka¹³¹, D. Cieri¹¹⁵, K. M. Ciesla⁸⁵, D. Cinca⁴⁷, V. Cindro⁹², I. A. Cioara^{27b}, A. Ciocio¹⁸, F. Ciroto^{70a,70b}, Z. H. Citron^{181.k}, M. Citterio^{69a}, D. A. Ciubotaru^{27b}, B. M. Ciungu¹⁶⁸, A. Clark⁵⁴, M. R. Clark³⁹, P. J. Clark⁵⁰, C. Clement^{45a,45b}, Y. Coadou¹⁰², M. Cobl^{67a,67c}, A. Coccaro^{55b}, J. Cochran⁷⁹, H. Cohen¹⁶², A. E. C. Coimbra³⁶, L. Colasurdo¹¹⁹, B. Cole³⁹, A. P. Colijn¹²⁰, J. Collot⁵⁸, P. Conde Muiño^{140a.f}, E. Coniavitis⁵², S. H. Connell^{33c}, I. A. Connelly⁵⁷, S. Constantinescu^{27b}, F. Conventi^{70a.ay}, A. M. Cooper-Sarkar¹³⁵, F. Cormier¹⁷⁶, K. J. R. Cormier¹⁶⁸, L. D. Corpe⁹⁵, M. Corradi^{73a,73b}, E. E. Corrigan⁹⁷, F. Corriveau^{104.af}, M. J. Costa¹⁷⁵, F. Costanza⁵, D. Costanzo¹⁵⁰, G. Cowan⁹⁴, J. W. Cowley³², J. Crane¹⁰¹, K. Cranmer¹²⁵, S. J. Crawley⁵⁷, R. A. Creager¹³⁷, S. Crépe-Renaudin⁵⁸, F. Crescioli¹³⁶, M. Cristinziani²⁴, V. Croft¹²⁰, G. Crosetti^{41b,41a}, A. Cueto⁵, T. Cuhadar Donszelmann¹⁵⁰, A. R. Cukierman¹⁵⁴, W. R. Cunningham⁵⁷, S. Czekierda⁸⁵, P. Czodrowski³⁶, M. J. Da Cunha Sargedas De Sousa^{60b}, J. V. Da Fonseca Pinto^{81b}, C. Da Via¹⁰¹, W. Dabrowski^{84a}, T. Dado^{28a}, S. Dahbi^{35e}, T. Dai¹⁰⁶, C. Dallapiccola¹⁰³, M. Dam⁴⁰, G. D'amen²⁹, V. D'Amico^{75a,75b}, J. Damp¹⁰⁰, J. R. Dandoy¹³⁷, M. F. Daneri³⁰, N. P. Dang^{182.j}, N. S. Dann¹⁰¹, M. Danninger¹⁷⁶, V. Dao³⁶, G. Darbo^{55b}, O. Dartsis⁵, A. Dattagupta¹³², T. Daubney⁴⁶, S. D'Auria^{69a,69b}, W. Davey²⁴, C. David⁴⁶, T. Davidek¹⁴³, D. R. Davis⁴⁹, I. Dawson¹⁵⁰, K. De⁸, R. De Asmundis^{70a}, M. De Beurs¹²⁰, S. De Castro^{23b,23a}, S. De Cecco^{73a,73b}, N. De Groot¹¹⁹, P. de Jong¹²⁰, H. De la Torre¹⁰⁷, A. De Maria^{15c}, D. De Pedis^{73a}, A. De Salvo^{73a}, U. De Sanctis^{74a,74b}, M. De Santis^{74a,74b}, A. De Santo¹⁵⁷, K. De Vasconcelos Corga¹⁰², J. B. De Vivie De Regie⁶⁵, C. Debenedetti¹⁴⁶, D. V. Dedovich⁸⁰, A. M. Deiana⁴², M. Del Gaudio^{41b,41a}, J. Del Peso⁹⁹, Y. Delabat Diaz⁴⁶, D. Delgove⁶⁵, F. Deliot^{145.r}, C. M. Delitzsch⁷, M. Della Pietra^{70a,70b}, D. Della Volpe⁵⁴, A. Dell'Acqua³⁶, L. Dell'Asta^{74a,74b}, M. Delmastro⁵, C. Delporte⁶⁵, P. A. Delsart⁵⁸, D. A. DeMarco¹⁶⁸, S. Demers¹⁸⁴, M. Demichev⁸⁰, G. Demontigny¹¹⁰, S. P. Denisov¹²³, D. Denysiuk¹²⁰, L. D'ErAMO¹³⁶, D. Derendarz⁸⁵, J. E. Derkaoui^{35d}, F. Derue¹³⁶, P. Dervan⁹¹, K. Desch²⁴, C. Deterre⁴⁶, K. Dette¹⁶⁸, C. Deutsch²⁴, M. R. Devesa³⁰, P. O. Deviveiros³⁶, A. Dewhurst¹⁴⁴, F. A. Di Bello⁵⁴, A. Di Ciaccio^{74a,74b}, L. Di Ciaccio⁵, W. K. Di Clemente¹³⁷, C. Di Donato^{70a,70b}, A. Di Girolamo³⁶

A. Guerguichon⁶⁵, J. G. R. Guerrero Rojas¹⁷⁵, F. Guescini¹¹⁵, D. Guest¹⁷², R. Gugel⁵², T. Guillemin⁵, S. Guindon³⁶, U. Gul⁵⁷, J. Guo^{60c}, W. Guo¹⁰⁶, Y. Guo^{60a}, Z. Guo¹⁰², R. Gupta⁴⁶, S. Gurbuz^{12c}, G. Gustavino¹²⁹, M. Guth⁵², P. Gutierrez¹²⁹, C. Gutsche⁹⁵, C. Guyot¹⁴⁵, C. Gwenlan¹³⁵, C. B. Gwilliam⁹¹, A. Haas¹²⁵, C. Haber¹⁸, H. K. Hadavand⁸, N. Haddad^{35e}, A. Hadeef^{60a}, S. Hageböck³⁶, M. Haleem¹⁷⁸, J. Haley¹³⁰, G. Halladjian¹⁰⁷, G. D. Hallewell¹⁰², K. Hamacher¹⁸³, P. Hamal¹³¹, K. Hamano¹⁷⁷, H. Hamdaoui^{35e}, G. N. Hamity¹⁵⁰, K. Han^{60a,z}, L. Han^{60a}, S. Han^{15a}, Y. F. Han¹⁶⁸, K. Hanagaki^{82,x}, M. Hance¹⁴⁶, D. M. Handl¹¹⁴, B. Haney¹³⁷, R. Hankache¹³⁶, E. Hansen⁹⁷, J. B. Hansen⁴⁰, J. D. Hansen⁴⁰, M. C. Hansen²⁴, P. H. Hansen⁴⁰, E. C. Hanson¹⁰¹, K. Hara¹⁷⁰, T. Harenberg¹⁸³, S. Harkusha¹⁰⁸, P. F. Harrison¹⁷⁹, N. M. Hartmann¹¹⁴, Y. Hasegawa¹⁵¹, A. Hasib⁵⁰, S. Hassani¹⁴⁵, S. Haug²⁰, R. Hauser¹⁰⁷, L. B. Havener³⁹, M. Havranek¹⁴², C. M. Hawkes²¹, R. J. Hawkins³⁶, D. Hayden¹⁰⁷, C. Hayes¹⁵⁶, R. L. Hayes¹⁷⁶, C. P. Hays¹³⁵, J. M. Hays⁹³, H. S. Hayward⁹¹, S. J. Haywood¹⁴⁴, F. He^{60a}, M. P. Heath⁵⁰, V. Hedberg⁹⁷, L. Heelan⁸, S. Heer²⁴, K. K. Heidegger⁵², W. D. Heidorn⁷⁹, J. Heilman³⁴, S. Heim⁴⁶, T. Heim¹⁸, B. Heinemann^{46.at}, J. J. Heinrich¹³², L. Heinrich³⁶, C. Heinz⁵⁶, J. Hejbal¹⁴¹, L. Helary^{61b}, A. Held¹⁷⁶, S. Hellesund¹³⁴, C. M. Helling¹⁴⁶, S. Hellman^{45a,45b}, C. Helsens³⁶, R. C. W. Henderson⁹⁰, Y. Heng¹⁸², S. Henkelmann¹⁷⁶, A. M. Henriques Correia³⁶, G. H. Herbert¹⁹, H. Herde²⁶, V. Herget¹⁷⁸, Y. Hernández Jiménez^{33e}, H. Herr¹⁰⁰, M. G. Herrmann¹¹⁴, T. Herrmann⁴⁸, G. Herten⁵², R. Hertenberger¹¹⁴, L. Hervas³⁶, T. C. Herwig¹³⁷, G. G. Hesketh⁹⁵, N. P. Hessey^{169a}, A. Higashida¹⁶⁴, S. Higashino⁸², E. Higón-Rodríguez¹⁷⁵, K. Hildebrand³⁷, E. Hill¹⁷⁷, J. C. Hill³², K. K. Hill²⁹, K. H. Hiller⁴⁶, S. J. Hillier²¹, M. Hils⁴⁸, I. Hinchliffe¹⁸, F. Hinterkeuser²⁴, M. Hirose¹³³, S. Hirose⁵², D. Hirschbuehl¹⁸³, B. Hiti⁹², O. Hladik¹⁴¹, D. R. Hlaluku^{33e}, X. Hoad⁵⁰, J. Hobbs¹⁵⁶, N. Hod¹⁸¹, M. C. Hodgkinson¹⁵⁰, A. Hoecker³⁶, F. Hoenic¹¹⁴, D. Hohn⁵², D. Hohov⁶⁵, T. R. Holmes³⁷, M. Holzbock¹¹⁴, L. B. A. H. Hommels³², S. Honda¹⁷⁰, T. M. Hong¹³⁹, J. C. Honig⁵², A. Hönle¹¹⁵, B. H. Hooberman¹⁷⁴, W. H. Hopkins⁶, Y. Horii¹¹⁷, P. Horn⁴⁸, L. A. Horyn³⁷, S. Hou¹⁵⁹, A. Hoummada^{35a}, J. Howarth¹⁰¹, J. Hoya⁸⁹, M. Hrabovsky¹³¹, J. Hrdinka⁷⁷, I. Hristova¹⁹, J. Hrivnac⁶⁵, A. Hrynevich¹⁰⁹, T. Hryn'ova⁵, P. J. Hsu⁶⁴, S.-C. Hsu¹⁴⁹, Q. Hu²⁹, S. Hu^{60c}, Y. F. Hu^{15a,15d}, D. P. Huang⁹⁵, Y. Huang^{60a}, Y. Huang^{15a}, Z. Hubacek¹⁴², F. Hubaut¹⁰², M. Huebner²⁴, F. Huegging²⁴, T. B. Huffman¹³⁵, M. Huhtinen³⁶, R. F. H. Hunter³⁴, P. Huo¹⁵⁶, A. M. Hupe³⁴, N. Huseynov^{80,ah}, J. Huston¹⁰⁷, J. Huth⁵⁹, R. Hyneman¹⁰⁶, S. Hyrych^{28a}, G. Iacobucci⁵⁴, G. Iakovidis²⁹, I. Ibragimov¹⁵², L. Iconomidou-Fayard⁶⁵, Z. Idrissi^{35e}, P. Iengo³⁶, R. Ignazzi⁴⁰, O. Igonkina^{120.ac,*}, R. Iguchi¹⁶⁴, T. Izawa⁵⁴, Y. Ikegami⁸², M. Ikeno⁸², D. Iliadis¹⁶³, N. Ilic^{119,168.af}, F. Iltzsche⁴⁸, G. Introzzi^{71a,71b}, M. Iodice^{75a}, K. Iordanidou^{169a}, V. Ippolito^{73a,73b}, M. F. Isacson¹⁷³, M. Ishino¹⁶⁴, W. Islam¹³⁰, C. Issever^{19,46}, S. Istin¹⁶¹, F. Ito¹⁷⁰, J. M. Iturbe Ponce^{63a}, R. Iuppa^{76a,76b}, A. Ivina¹⁸¹, H. Iwasaki⁸², J. M. Izen⁴³, V. Izzo^{70a}, P. Jacka¹⁴¹, P. Jackson¹, R. M. Jacobs²⁴, B. P. Jaeger¹⁵³, V. Jain², G. Jäkel¹⁸³, K. B. Jakobi¹⁰⁰, K. Jakobs⁵², T. Jakoubek¹⁴¹, J. Jamieson⁵⁷, K. W. Janas^{84a}, R. Jansky⁵⁴, J. Janssen²⁴, M. Janus⁵³, P. A. Janus^{84a}, G. Jarlskog⁹⁷, N. Javadov^{80,ah}, T. Javůrek³⁶, M. Javurkova⁵², F. Jeanneau¹⁴⁵, L. Jeanty¹³², J. Jejelava^{160a.ai}, A. Jelinskas¹⁷⁹, P. Jenni^{52,b}, J. Jeong⁴⁶, N. Jeong⁴⁶, S. Jézéquel⁵, H. Ji¹⁸², J. Jia¹⁵⁶, H. Jiang⁷⁹, Y. Jiang^{60a}, Z. Jiang^{154,q}, S. Jiggins⁵², F. A. Jimenez Morales³⁸, J. Jimenez Pena¹¹⁵, S. Jin^{15c}, A. Jinaru^{27b}, O. Jinnouchi¹⁶⁶, H. Jivan^{33e}, P. Johansson¹⁵⁰, K. A. Johns⁷, C. A. Johnson⁶⁶, K. Jon-And^{45a,45b}, R. W. L. Jones⁹⁰, S. D. Jones¹⁵⁷, S. Jones⁷, T. J. Jones⁹¹, J. Jongmanns^{61a}, P. M. Jorge^{140a}, J. Jovicevic³⁶, X. Ju¹⁸, J. J. Junggeburth¹¹⁵, A. Juste Rozas^{14,aa}, A. Kaczmarska⁸⁵, M. Kado^{73a,73b}, H. Kagan¹²⁷, M. Kagan¹⁵⁴, A. Kahn³⁹, C. Kahra¹⁰⁰, T. Kaji¹⁸⁰, E. Kajomovitz¹⁶¹, C. W. Kalderon⁹⁷, A. Kaluza¹⁰⁰, A. Kamenshchikov¹²³, M. Kaneda¹⁶⁴, L. Kanjir⁹², Y. Kano¹¹⁷, V. A. Kantserov¹¹², J. Kanzaki⁸², L. S. Kaplan¹⁸², D. Kar^{33e}, K. Karava¹³⁵, M. J. Kareem^{169b}, S. N. Karpov⁸⁰, Z. M. Karpova⁸⁰, V. Kartvelishvili⁹⁰, A. N. Karyukhin¹²³, L. Kashif¹⁸², R. D. Kass¹²⁷, A. Kastanas^{45a,45b}, C. Kato^{60d,60c}, J. Katzy⁴⁶, K. Kawade¹⁵¹, K. Kawagoe⁸⁸, T. Kawaguchi¹¹⁷, T. Kawamoto¹⁶⁴, G. Kawamura⁵³, E. F. Kay¹⁷⁷, V. F. Kazanin^{122b,122a}, R. Keeler¹⁷⁷, R. Kehoe⁴², J. S. Keller³⁴, E. Kellermann⁹⁷, D. Kelsey¹⁵⁷, J. J. Kempster²¹, J. Kendrick²¹, K. E. Kennedy³⁹, O. Kepka¹⁴¹, S. Kersten¹⁸³, B. P. Kerševan⁹², S. Ketabchi Haghighat¹⁶⁸, M. Khader¹⁷⁴, F. Khalil-Zada¹³, M. Khandoga¹⁴⁵, A. Khanov¹³⁰, A. G. Kharlamov^{122b,122a}, T. Kharlamova^{122b,122a}, E. E. Khoda¹⁷⁶, A. Khodinov¹⁶⁷, T. J. Khoo⁵⁴, E. Khramov⁸⁰, J. Khubua^{160b}, S. Kido⁸³, M. Kiehn⁵⁴, C. R. Kilby⁹⁴, Y. K. Kim³⁷, N. Kimura⁹⁵, O. M. Kind¹⁹, B. T. King^{91,*}, D. Kirchmeier⁴⁸, J. Kirk¹⁴⁴, A. E. Kiryunin¹¹⁵, T. Kishimoto¹⁶⁴, D. P. Kisliuk¹⁶⁸, V. Kitali⁴⁶, O. Kivernyk⁵, T. Klapdor-Kleingrothaus⁵², M. Klassen^{61a}, M. H. Klein¹⁰⁶, M. Klein⁹¹, U. Klein⁹¹, K. Kleinknecht¹⁰⁰, P. Klimek¹²¹, A. Klimentov²⁹, T. Klingl²⁴, T. Klioutchnikova³⁶, F. F. Klitzner¹¹⁴, P. Kluit¹²⁰, S. Kluth¹¹⁵, E. Kneringer⁷⁷, E. B. F. G. Knoop¹⁰², A. Knue⁵², D. Kobayashi⁸⁸, T. Kobayashi¹⁶⁴, M. Kobel⁴⁸, M. Kocian¹⁵⁴, P. Kodys¹⁴³, P. T. Koenig²⁴

T. Koffas³⁴, N. M. Köhler³⁶, T. Koi¹⁵⁴, M. Kolb^{61b}, I. Koletsou⁵, T. Komarek¹³¹, T. Kondo⁸², N. Kondrashova^{60c}, K. Köneke⁵², A. C. König¹¹⁹, T. Kono¹²⁶, R. Konoplich^{125,ao}, V. Konstantinides⁹⁵, N. Konstantinidis⁹⁵, B. Konya⁹⁷, R. Kopeliansky⁶⁶, S. Koperny^{84a}, K. Korcyl⁸⁵, K. Kordas¹⁶³, G. Koren¹⁶², A. Korn⁹⁵, I. Korolkov¹⁴, E. V. Korolkova¹⁵⁰, N. Korotkova¹¹³, O. Kortner¹¹⁵, S. Kortner¹¹⁵, T. Kosek¹⁴³, V. V. Kostyukhin¹⁶⁷, A. Kotsokechagia⁶⁵, A. Kotwal⁴⁹, A. Koulouris¹⁰, A. Kourkouveli-Charalampidi^{71a,71b}, C. Kourkoumelis⁹, E. Kourlitis¹⁵⁰, V. Kouskoura²⁹, A. B. Kowalewska⁸⁵, R. Kowalewski¹⁷⁷, C. Kozakai¹⁶⁴, W. Kozanecki¹⁴⁵, A. S. Kozhin¹²³, V. A. Kramarenko¹¹³, G. Kramberger⁹², D. Krasnopevtsev^{60a}, M. W. Krasny¹³⁶, A. Krasznahorkay³⁶, D. Krauss¹¹⁵, J. A. Kremer^{84a}, J. Kretzschmar⁹¹, P. Krieger¹⁶⁸, F. Krieter¹¹⁴, A. Krishnan^{61b}, K. Krizka¹⁸, K. Kroeninger⁴⁷, H. Kroha¹¹⁵, J. Kroll¹⁴¹, J. Kroll¹³⁷, K. S. Krowpman¹⁰⁷, J. Krstic¹⁶, U. Kruchonak⁸⁰, H. Krüger²⁴, N. Krumnack⁷⁹, M. C. Kruse⁴⁹, J. A. Krzysiak⁸⁵, T. Kubota¹⁰⁵, O. Kuchinskaja¹⁶⁷, S. Kudah^{4b}, D. Kuechler⁴⁶, J. T. Kuechler⁴⁶, S. Kuehn³⁶, A. Kugel^{61a}, T. Kuhl⁴⁶, V. Kukhtin⁸⁰, R. Kukla¹⁰², Y. Kulchitsky^{108,al}, S. Kuleshov^{147d}, Y. P. Kulinich¹⁷⁴, M. Kuna⁵⁸, T. Kunigo⁸⁶, A. Kupco¹⁴¹, T. Kupfer⁴⁷, O. Kuprash⁵², H. Kurashige⁸³, L. L. Kurchaninov^{169a}, Y. A. Kurochkin¹⁰⁸, A. Kurova¹¹², M. G. Kurth^{15a,15d}, E. S. Kuwertz³⁶, M. Kuze¹⁶⁶, A. K. Kvam¹⁴⁹, J. Kvita¹³¹, T. Kwan¹⁰⁴, A. La Rosa¹¹⁵, L. La Rotonda^{41b,41a}, F. La Ruffa^{41b,41a}, C. Lacasta¹⁷⁵, F. Lacava^{73a,73b}, D. P. J. Lack¹⁰¹, H. Lacker¹⁹, D. Lacour¹³⁶, E. Ladygin⁸⁰, R. Lafaye⁵, B. Laforge¹³⁶, T. Lagouri^{33e}, S. Lai⁵³, S. Lammers⁶⁶, W. Lampl⁷, C. Lampoudis¹⁶³, E. Lançon²⁹, U. Landgraf⁵², M. P. J. Landon⁹³, M. C. Lanfermann⁵⁴, V. S. Lang⁴⁶, J. C. Lange⁵³, R. J. Langenberg³⁶, A. J. Lankford¹⁷², F. Lanni²⁹, K. Lantzschi²⁴, A. Lanza^{71a}, A. Lapertosa^{55b,55a}, S. Laplace¹³⁶, J. F. Laporte¹⁴⁵, T. Lari^{69a}, F. Lasagni Manghi^{23b,23a}, M. Lassnig³⁶, T. S. Lau^{63a}, A. Laudrain⁶⁵, A. Laurier³⁴, M. Lavorgna^{70a,70b}, S. D. Lawlor⁹⁴, M. Lazzaroni^{69a,69b}, B. Le¹⁰⁵, E. Le Guirriec¹⁰², M. LeBlanc⁷, T. LeCompte⁶, F. Ledroit-Guillon⁵⁸, A. C. A. Lee⁹⁵, C. A. Lee²⁹, G. R. Lee¹⁷, L. Lee⁵⁹, S. C. Lee¹⁵⁹, S. J. Lee³⁴, S. Lee⁷⁹, B. Lefebvre^{169a}, H. P. Lefebvre⁹⁴, M. Lefebvre¹⁷⁷, F. Legger¹¹⁴, C. Leggett¹⁸, K. Lehmann¹⁵³, N. Lehmann¹⁸³, G. Lehmann Miotto³⁶, W. A. Leight⁴⁶, A. Leisos^{163,y}, M. A. L. Leite^{81c}, C. E. Leitgeb¹¹⁴, R. Leitner¹⁴³, D. Lellouch^{181,*}, K. J. C. Leney⁴², T. Lenz²⁴, B. Lenzi³⁶, R. Leone⁷, S. Leone^{72a}, C. Leonidopoulos⁵⁰, A. Leopold¹³⁶, G. Lerner¹⁵⁷, C. Leroy¹¹⁰, R. Les¹⁶⁸, C. G. Lester³², M. Levchenko¹³⁸, J. Levêque⁵, D. Levin¹⁰⁶, L. J. Levinson¹⁸¹, D. J. Lewis²¹, B. Li^{15b}, B. Li¹⁰⁶, C.-Q. Li^{60a}, F. Li^{60c}, H. Li^{60a}, H. Li^{60b}, J. Li^{60c}, K. Li¹⁵⁴, L. Li^{60c}, M. Li^{15a,15d}, Q. Li^{15a,15d}, Q. Y. Li^{60a}, S. Li^{60d,60c}, X. Li⁴⁶, Y. Li⁴⁶, Z. Li^{60b}, Z. Liang^{15a}, B. Liberti^{74a}, A. Liblong¹⁶⁸, K. Lie^{63c}, S. Lim²⁹, C. Y. Lin³², K. Lin¹⁰⁷, T. H. Lin¹⁰⁰, R. A. Linck⁶⁶, J. H. Lindon²¹, A. L. Lioni⁵⁴, E. Lipeles¹³⁷, A. Lipniacka¹⁷, M. Lisovsky^{61b}, T. M. Liss^{174,av}, A. Lister¹⁷⁶, A. M. Litke¹⁴⁶, J. D. Little⁸, B. Liu⁷⁹, B. X. Liu⁶, H. B. Liu²⁹, H. Liu¹⁰⁶, J. B. Liu^{60a}, J. K. K. Liu¹³⁵, K. Liu¹³⁶, M. Liu^{60a}, P. Liu¹⁸, Y. Liu^{15a,15d}, Y. L. Liu¹⁰⁶, Y. W. Liu^{60a}, M. Livan^{71a,71b}, A. Lleres⁵⁸, J. Llorente Merino¹⁵³, S. L. Lloyd⁹³, C. Y. Lo^{63b}, F. Lo Sterzo⁴², E. M. Lobodzinska⁴⁶, P. Loch⁷, S. Loffredo^{74a,74b}, T. Lohse¹⁹, K. Lohwasser¹⁵⁰, M. Lokajicek¹⁴¹, J. D. Long¹⁷⁴, R. E. Long⁹⁰, L. Longo³⁶, K. A. Looper¹²⁷, J. A. Lopez^{147d}, I. Lopez Paz¹⁰¹, A. Lopez Solis¹⁵⁰, J. Lorenz¹¹⁴, N. Lorenzo Martinez⁵, M. Losada^{22a}, P. J. Lösel¹¹⁴, A. Lösle⁵², X. Lou⁴⁶, X. Lou^{15a}, A. Lounis⁶⁵, J. Love⁶, P. A. Love⁹⁰, J. J. Lozano Bahilo¹⁷⁵, M. Lu^{60a}, Y. J. Lu⁶⁴, H. J. Lubatti¹⁴⁹, C. Luci^{73a,73b}, A. Lucotte⁵⁸, C. Luedtke⁵², F. Luehring⁶⁶, I. Luise¹³⁶, L. Luminari^{73a}, B. Lund-Jensen¹⁵⁵, M. S. Lutz¹⁰³, D. Lynn²⁹, H. Lyons⁹¹, R. Lysak¹⁴¹, E. Lytken⁹⁷, F. Lyu^{15a}, V. Lyubushkin⁸⁰, T. Lyubushkina⁸⁰, H. Ma²⁹, L. L. Ma^{60b}, Y. Ma^{60b}, G. Maccarrone⁵¹, A. Macchiolo¹¹⁵, C. M. Macdonald¹⁵⁰, J. Machado Miguens¹³⁷, D. Madaffari¹⁷⁵, R. Madar³⁸, W. F. Mader⁴⁸, N. Madysa⁴⁸, J. Maeda⁸³, T. Maeno²⁹, M. Maerker⁴⁸, A. S. Maevskiy¹¹³, V. Magerl⁵², N. Magini⁷⁹, D. J. Mahon³⁹, C. Maidantchik^{81b}, T. Maier¹¹⁴, A. Maio^{140a,140b,140d}, K. Maj^{84a}, O. Majersky^{28a}, S. Majewski¹³², Y. Makida⁸², N. Makovec⁶⁵, B. Malaescu¹³⁶, Pa. Malecki⁸⁵, V. P. Maleev¹³⁸, F. Malek⁵⁸, U. Mallik⁷⁸, D. Malon⁶, C. Malone³², S. Maltezos¹⁰, S. Malyukov⁸⁰, J. Mamuzic¹⁷⁵, G. Mancini⁵¹, I. Mandić⁹², L. Manhaes de Andrade Filho^{81a}, I. M. Maniatis¹⁶³, J. Manjarres Ramos⁴⁸, K. H. Mankinen⁹⁷, A. Mann¹¹⁴, A. Manousos⁷⁷, B. Mansoulie¹⁴⁵, I. Manthos¹⁶³, S. Manzoni¹²⁰, A. Marantis¹⁶³, G. Marceca³⁰, L. Marchese¹³⁵, G. Marchioni¹³⁶, M. Marcisovsky¹⁴¹, L. Marcocchia^{74a,74b}, C. Marcon⁹⁷, C. A. Marin Tobon³⁶, M. Marjanovic¹²⁹, Z. Marshall¹⁸, M. U. F. Martensson¹⁷³, S. Marti-Garcia¹⁷⁵, C. B. Martin¹²⁷, T. A. Martin¹⁷⁹, V. J. Martin⁵⁰, B. Martin dit Latour¹⁷, L. Martinelli^{75a,75b}, M. Martinez^{14,aa}, V. I. Martinez Outschoorn¹⁰³, S. Martin-Haugh¹⁴⁴, V. S. Martouiu^{27b}, A. C. Martyniuk⁹⁵, A. Marzin³⁶, S. R. Maschek¹¹⁵, L. Masetti¹⁰⁰, T. Mashimo¹⁶⁴, R. Mashinistov¹¹¹, J. Masik¹⁰¹, A. L. Maslennikov^{122b,122a}, L. Massa^{74a,74b}, P. Massarotti^{70a,70b}, P. Mastrandrea^{72a,72b}, A. Mastroberardino^{41b,41a}, T. Masubuchi¹⁶⁴, D. Matakias¹⁰, A. Matic¹¹⁴, P. Mättig²⁴

J. Maurer^{27b}, B. Maček⁹², D. A. Maximov^{122b,122a}, R. Mazini¹⁵⁹, I. Maznas¹⁶³, S. M. Mazza¹⁴⁶, S. P. Mc Kee¹⁰⁶, T. G. McCarthy¹¹⁵, W. P. McCormack¹⁸, E. F. McDonald¹⁰⁵, J. A. Mcfayden³⁶, G. Mchedlidze^{160b}, M. A. McKay⁴², K. D. McLean¹⁷⁷, S. J. McMahon¹⁴⁴, P. C. McNamara¹⁰⁵, C. J. McNicol¹⁷⁹, R. A. McPherson^{177.af}, J. E. Mdhluli^{33e}, Z. A. Meadows¹⁰³, S. Meehan³⁶, T. Megy⁵², S. Mehlhase¹¹⁴, A. Mehta⁹¹, T. Meideck⁵⁸, B. Meirose⁴³, D. Melini¹⁷⁵, B. R. Mellado Garcia^{33e}, J. D. Mellenthin⁵³, M. Melo^{28a}, F. Meloni⁴⁶, A. Melzer²⁴, S. B. Menary¹⁰¹, E. D. Mendes Gouveia^{140a,140e}, L. Meng³⁶, X. T. Meng¹⁰⁶, S. Menke¹¹⁵, E. Meoni^{41b,41a}, S. Mergelmeyer¹⁹, S. A. M. Merkt¹³⁹, C. Merlassino²⁰, P. Mermod⁵⁴, L. Merola^{70a,70b}, C. Meroni^{69a}, O. Meshkov^{113,111}, J. K. R. Meshreki¹⁵², A. Messina^{73a,73b}, J. Metcalfe⁶, A. S. Mete¹⁷², C. Meyer⁶⁶, J. Meyer¹⁶¹, J.-P. Meyer¹⁴⁵, H. Meyer Zu Theenhausen^{61a}, F. Miano¹⁵⁷, M. Michetti¹⁹, R. P. Middleton¹⁴⁴, L. Mijović⁵⁰, G. Mikenberg¹⁸¹, M. Mikestikova¹⁴¹, M. Mikuž⁹², H. Mildner¹⁵⁰, M. Milesi¹⁰⁵, A. Milic¹⁶⁸, D. A. Millar⁹³, D. W. Miller³⁷, A. Milov¹⁸¹, D. A. Milstead^{45a,45b}, R. A. Mina^{154.q}, A. A. Minaenko¹²³, M. Miñano Moya¹⁷⁵, I. A. Minashvili^{160b}, A. I. Mincer¹²⁵, B. Mindur^{84a}, M. Mineev⁸⁰, Y. Minegishi¹⁶⁴, L. M. Mir¹⁴, A. Mirtó^{68a,68b}, K. P. Mistry¹³⁷, T. Mitani¹⁸⁰, J. Mitrevski¹¹⁴, V. A. Mitsou¹⁷⁵, M. Mittal^{60c}, O. Miu¹⁶⁸, A. Miucci²⁰, P. S. Miyagawa¹⁵⁰, A. Mizukami⁸², J. U. Mjörnmark⁹⁷, T. Mkrtychyan¹⁸⁵, M. Mlynarikova¹⁴³, T. Moa^{45a,45b}, K. Mochizuki¹¹⁰, P. Mogg⁵², S. Mohapatra³⁹, R. Moles-Valls²⁴, M. C. Mondragon¹⁰⁷, K. Mönig⁴⁶, J. Monk⁴⁰, E. Monnier¹⁰², A. Montalbano¹⁵³, J. Montejo Berlingen³⁶, M. Montella⁹⁵, F. Monticelli⁸⁹, S. Monzani^{69a}, N. Morange⁶⁵, D. Moreno^{22a}, M. Moreno Llácer¹⁷⁵, C. Moreno Martinez¹⁴, P. Moretini^{55b}, M. Morgenstern¹²⁰, S. Morgenstern⁴⁸, D. Mori¹⁵³, M. Morii⁵⁹, M. Morinaga¹⁸⁰, V. Morisbak¹³⁴, A. K. Morley³⁶, G. Mornacchi³⁶, A. P. Morris⁹⁵, L. Morvaj¹⁵⁶, P. Moschovakos³⁶, B. Moser¹²⁰, M. Mosidze^{160b}, T. Moskalets¹⁴⁵, H. J. Moss¹⁵⁰, J. Moss^{31,n}, E. J. W. Moyse¹⁰³, S. Muanza¹⁰², J. Mueller¹³⁹, R. S. P. Mueller¹¹⁴, D. Muenstermann⁹⁰, G. A. Mullier⁹⁷, D. P. Mungo^{69a,69b}, J. L. Munoz Martinez¹⁴, F. J. Munoz Sanchez¹⁰¹, P. Murin^{28b}, W. J. Murray^{179,144}, A. Murrone^{69a,69b}, M. Muškinja¹⁸, C. Mwewa^{33a}, A. G. Myagkov^{123.ap}, J. Myers¹³², M. Myska¹⁴², B. P. Nachman¹⁸, O. Nackenhörst⁴⁷, A. Nag Nag⁴⁸, K. Nagai¹³⁵, K. Nagano⁸², Y. Nagasaka⁶², M. Nagel⁵², J. L. Nagle²⁹, E. Nagy¹⁰², A. M. Nairz³⁶, Y. Nakahama¹¹⁷, K. Nakamura⁸², T. Nakamura¹⁶⁴, I. Nakano¹²⁸, H. Nanjo¹³³, F. Napolitano^{61a}, R. F. Naranjo Garcia⁴⁶, R. Narayan⁴², I. Naryshkin¹³⁸, T. Naumann⁴⁶, G. Navarro^{22a}, P. Y. Nechaeva¹¹¹, F. Nechansky⁴⁶, T. J. Neep²¹, A. Negri^{71a,71b}, M. Negrini^{23b}, C. Nellist⁵³, M. E. Nelson¹³⁵, S. Nemecek¹⁴¹, P. Nemethy¹²⁵, M. Nessi^{36.d}, M. S. Neubauer¹⁷⁴, M. Neumann¹⁸³, P. R. Newman²¹, Y. S. Ng¹⁹, Y. W. Y. Ng¹⁷², B. Ngair^{35e}, H. D. N. Nguyen¹⁰², T. Nguyen Manh¹¹⁰, E. Nibigira³⁸, R. B. Nickerson¹³⁵, R. Nicolaidou¹⁴⁵, D. S. Nielsen⁴⁰, J. Nielsen¹⁴⁶, N. Nikiforou¹¹, V. Nikolaenko^{123.ap}, I. Nikolic-Audit¹³⁶, K. Nikolopoulos²¹, P. Nilsson²⁹, H. R. Nindhito⁵⁴, Y. Ninomiya⁸², A. Nisati^{73a}, N. Nishu^{60c}, R. Nisius¹¹⁵, I. Nitsche⁴⁷, T. Nitta¹⁸⁰, T. Nobe¹⁶⁴, Y. Noguchi⁸⁶, I. Nomidis¹³⁶, M. A. Nomura²⁹, M. Nordberg³⁶, N. Norjoharuddeen¹³⁵, T. Novak⁹², O. Novgorodova⁴⁸, R. Novotny¹⁴², L. Nozka¹³¹, K. Ntekas¹⁷², E. Nurse⁹⁵, F. G. Oakham^{34.ax}, H. Oberlack¹¹⁵, J. Ocariz¹³⁶, A. Ochi⁸³, I. Ochoa³⁹, J. P. Ochoa-Ricoux^{147a}, K. O'Connor²⁶, S. Oda⁸⁸, S. Odaka⁸², S. Oerdek⁵³, A. Ogrodnik^{84a}, A. Oh¹⁰¹, S. H. Oh⁴⁹, C. C. Ohm¹⁵⁵, H. Oide¹⁶⁶, M. L. Ojeda¹⁶⁸, H. Okawa¹⁷⁰, Y. Okazaki⁸⁶, M. W. O'Keefe⁹¹, Y. Okumura¹⁶⁴, T. Okuyama⁸², A. Olariu^{27b}, L. F. Oleiro Seabra^{140a}, S. A. Olivares Pino^{147a}, D. Oliveira Damazio²⁹, J. L. Oliver¹, M. J. R. Olsson¹⁷², A. Olszewski⁸⁵, J. Olszowska⁸⁵, D. C. O'Neill¹⁵³, A. P. O'Neill¹³⁵, A. Onofre^{140a,140e}, P. U. E. Onyisi¹¹, H. Oppen¹³⁴, M. J. Oreglia³⁷, G. E. Orellana⁸⁹, D. Orestano^{75a,75b}, N. Orlando¹⁴, R. S. Orr¹⁶⁸, V. O'Shea⁵⁷, R. Ospanov^{60a}, G. Otero y Garzon³⁰, H. Otono⁸⁸, P. S. Ott^{61a}, M. Ouchrif^{35d}, J. Ouellette²⁹, F. Ould-Saada¹³⁴, A. Ouraou^{145.*}, Q. Ouyang^{15a}, M. Owen⁵⁷, R. E. Owen²¹, V. E. Ozcan^{12c}, N. Ozturk⁸, J. Pacalt¹³¹, H. A. Pacey³², K. Pachal⁴⁹, A. Pacheco Pages¹⁴, C. Padilla Aranda¹⁴, S. Pagan Griso¹⁸, M. Paganini¹⁸⁴, G. Palacino⁶⁶, S. Palazzo⁵⁰, S. Palestini³⁶, M. Palka^{84b}, D. Pallin³⁸, I. Panagoulas¹⁰, C. E. Pandini³⁶, J. G. Panduro Vazquez⁹⁴, P. Pani⁴⁶, G. Panizzo^{67a,67c}, L. Paolozzi⁵⁴, C. Papadatos¹¹⁰, K. Papageorgiou^{9,h}, S. Parajuli⁴³, A. Paramonov⁶, D. Paredes Hernandez^{63b}, S. R. Paredes Saenz¹³⁵, B. Parida¹⁶⁷, T. H. Park¹⁶⁸, A. J. Parker³¹, M. A. Parker³², F. Parodi^{55b,55a}, E. W. Parrish¹²¹, J. A. Parsons³⁹, U. Parzefall⁵², L. Pascual Dominguez¹³⁶, V. R. Pascuzzi¹⁶⁸, J. M. P. Pasner¹⁴⁶, F. Pasquali¹²⁰, E. Pasqualucci^{73a}, S. Passaggio^{55b}, F. Pastore⁹⁴, P. Pasuwan^{45a,45b}, S. Pataraja¹⁰⁰, J. R. Pater¹⁰¹, A. Pathak^{182.j}, T. Pauly³⁶, B. Pearson¹¹⁵, M. Pedersen¹³⁴, L. Pedraza Diaz¹¹⁹, R. Pedro^{140a}, T. Peiffer⁵³, S. V. Peleganchuk^{122b,122a}, O. Penc¹⁴¹, H. Peng^{60a}, B. S. Peralva^{81a}, M. M. Perego⁶⁵, A. P. Pereira Peixoto^{140a}, D. V. Perepelitsa²⁹, F. Peri¹⁹, L. Perini^{69a,69b}, H. Pernegger³⁶, S. Perrella^{70a,70b}, K. Peters⁴⁶, R. F. Y. Peters¹⁰¹, B. A. Petersen³⁶, T. C. Petersen⁴⁰, E. Petit¹⁰², A. Petridis¹, C. Petridou¹⁶³, M. Petrov¹³⁵, F. Petrucci^{75a,75b}, M. Pettee¹⁸⁴, N. E. Pettersson¹⁰³, K. Petukhova¹⁴³

A. Peyaud¹⁴⁵, R. Pezoa^{147d}, L. Pezzotti^{71a,71b}, T. Pham¹⁰⁵, F. H. Phillips¹⁰⁷, P. W. Phillips¹⁴⁴, M. W. Phipps¹⁷⁴, G. Piacquadio¹⁵⁶, E. Pianori¹⁸, A. Picazio¹⁰³, R. H. Pickles¹⁰¹, R. Piegaia³⁰, D. Pietreanu^{27b}, J. E. Pilcher³⁷, A. D. Pilkington¹⁰¹, M. Pinamonti^{74a,74b}, J. L. Pinfold³, M. Pitt¹⁶², L. Pizzimento^{74a,74b}, M.-A. Pleier²⁹, V. Pleskot¹⁴³, E. Plotnikova⁸⁰, P. Podberczko^{122b,122a}, R. Poettgen⁹⁷, R. Poggi⁵⁴, L. Poggioli⁶⁵, I. Pogrebnyak¹⁰⁷, D. Pohl²⁴, I. Pokharel⁵³, G. Polesello^{71a}, A. Poley¹⁸, A. Policicchio^{73a,73b}, R. Polifka¹⁴³, A. Polini^{23b}, C. S. Pollard⁴⁶, V. Polychronakos²⁹, D. Ponomarenko¹¹², L. Pontecorvo³⁶, S. Popa^{27a}, G. A. Popeneciu^{27d}, L. Portales⁵, D. M. Portillo Quintero⁵⁸, S. Pospisil¹⁴², K. Potamianos⁴⁶, I. N. Potrap⁸⁰, C. J. Potter³², H. Potti¹¹, T. Poulsen⁹⁷, J. Poveda³⁶, T. D. Powell¹⁵⁰, G. Pownall⁴⁶, M. E. Pozo Astigarraga³⁶, P. Pralavorio¹⁰², S. Prell⁷⁹, D. Price¹⁰¹, M. Primavera^{68a}, S. Prince¹⁰⁴, M. L. Proffitt¹⁴⁹, N. Proklova¹¹², K. Prokofiev^{63c}, F. Prokoshin⁸⁰, S. Protopopescu²⁹, J. Proudfoot⁶, M. Przybycien^{84a}, D. Pudza¹³⁸, A. Puri¹⁷⁴, P. Puzo⁶⁵, J. Qian¹⁰⁶, Y. Qin¹⁰¹, A. Quadt⁵³, M. Queitsch-Maitland⁴⁶, A. Qureshi¹, M. Racko^{28a}, P. Rados¹⁰⁵, F. Ragusa^{69a,69b}, G. Rahal⁹⁸, J. A. Raine⁵⁴, S. Rajagopalan²⁹, A. Ramirez Morales⁹³, K. Ran^{15a,15d}, T. Rashid⁶⁵, S. Raspopov⁵, D. M. Rauch⁴⁶, F. Rauscher¹¹⁴, S. Rave¹⁰⁰, B. Ravina¹⁵⁰, I. Ravinovich¹⁸¹, J. H. Rawling¹⁰¹, M. Raymond³⁶, A. L. Read¹³⁴, N. P. Readioff⁵⁸, M. Reale^{68a,68b}, D. M. Rebuffi^{71a,71b}, A. Redelbach¹⁷⁸, G. Redlinger²⁹, K. Reeves⁴³, L. Rehnisch¹⁹, J. Reichert¹³⁷, D. Reikher¹⁶², A. Reiss¹⁰⁰, A. Rej¹⁵², C. Rembser³⁶, M. Renda^{27b}, M. Rescigno^{73a}, S. Resconi^{69a}, E. D. Resseguie¹³⁷, S. Rettie¹⁷⁶, E. Reynolds²¹, O. L. Rezanova^{122b,122a}, P. Reznicek¹⁴³, E. Ricci^{76a,76b}, R. Richter¹¹⁵, S. Richter⁴⁶, E. Richter-Was^{84b}, O. Ricken²⁴, M. Ridel¹³⁶, P. Rieck¹¹⁵, O. Rifki⁴⁶, M. Rijssenbeek¹⁵⁶, A. Rimoldi^{71a,71b}, M. Rimoldi⁴⁶, L. Rinaldi^{23b}, G. Ripellino¹⁵⁵, I. Riu¹⁴, J. C. Rivera Vergara¹⁷⁷, F. Rizatdinova¹³⁰, E. Rizvi⁹³, C. Rizzi³⁶, R. T. Roberts¹⁰¹, S. H. Robertson^{104,af}, M. Robin⁴⁶, D. Robinson³², J. E. M. Robinson⁴⁶, C. M. Robles Gajardo^{147d}, A. Robson⁵⁷, A. Rocchi^{74a,74b}, E. Rocco¹⁰⁰, C. Roda^{72a,72b}, S. Rodriguez Bosca¹⁷⁵, A. Rodriguez Perez¹⁴, D. Rodriguez Rodriguez¹⁷⁵, A. M. Rodríguez Vera^{169b}, S. Roe³⁶, O. Röhne¹³⁴, R. Röhrig¹¹⁵, R. A. Rojas^{147d}, C. P. A. Roland⁶⁶, J. Roloff²⁹, A. Romaniouk¹¹², M. Romano^{23b,23a}, N. Rompotis⁹¹, M. Ronzani¹²⁵, L. Roos¹³⁶, S. Rosati^{73a}, K. Rosbach⁵², G. Rosin¹⁰³, B. J. Rosser¹³⁷, E. Rossi⁴⁶, E. Rossi^{75a,75b}, E. Rossi^{70a,70b}, L. P. Rossi^{55b}, L. Rossini^{69a,69b}, R. Rosten¹⁴, M. Rotaru^{27b}, J. Rothberg¹⁴⁹, D. Rousseau⁶⁵, G. Rovelli^{71a,71b}, A. Roy¹¹, D. Roy^{33e}, A. Rozanov¹⁰², Y. Rozen¹⁶¹, X. Ruan^{33e}, F. Rühr⁵², A. Ruiz-Martinez¹⁷⁵, A. Rummeler³⁶, Z. Rurikova⁵², N. A. Rusakovich⁸⁰, H. L. Russell¹⁰⁴, L. Rustige^{38,47}, J. P. Rutherford⁷, E. M. Rüttinger¹⁵⁰, M. Rybar³⁹, G. Rybkin⁶⁵, E. B. Rye¹³⁴, A. Ryzhov¹²³, J. A. Sabater Iglesias⁴⁶, P. Sabatini⁵³, G. Sabato¹²⁰, S. Sacerdoti⁶⁵, H.F.-W. Sadrozinski¹⁴⁶, R. Sadykov⁸⁰, F. Safai Tehrani^{73a}, B. Safarzadeh Samani¹⁵⁷, P. Saha¹²¹, S. Saha¹⁰⁴, M. Sahinsoy^{61a}, A. Sahu¹⁸³, M. Saimpert⁴⁶, M. Saito¹⁶⁴, T. Saito¹⁶⁴, H. Sakamoto¹⁶⁴, A. Sakharov^{125,ao}, D. Salamani⁵⁴, G. Salamanna^{75a,75b}, J. E. Salazar Loyola^{147d}, A. Salnikov¹⁵⁴, J. Salt¹⁷⁵, D. Salvatore^{41b,41a}, F. Salvatore¹⁵⁷, A. Salvucci^{63a,63b,63c}, A. Salzburger³⁶, J. Samarati³⁶, D. Sammel⁵², D. Sampsonidis¹⁶³, D. Sampsonidou¹⁶³, J. Sánchez¹⁷⁵, A. Sanchez Pineda^{67a,36,67c}, H. Sandaker¹³⁴, C. O. Sander⁴⁶, I. G. Sanderswood⁹⁰, M. Sandhoff¹⁸³, C. Sandoval^{22a}, D. P. C. Sankey¹⁴⁴, M. Sannino^{55b,55a}, Y. Sano¹¹⁷, A. Sansoni⁵¹, C. Santoni³⁸, H. Santos^{140a,140b}, S. N. Santpur¹⁸, A. Santra¹⁷⁵, A. Saponov⁸⁰, J. G. Saraiva^{140a,140d}, O. Sasaki⁸², K. Sato¹⁷⁰, F. Sauerburger⁵², E. Sauvan⁵, P. Savard^{168,ax}, N. Savic¹¹⁵, R. Sawada¹⁶⁴, C. Sawyer¹⁴⁴, L. Sawyer^{96,am}, C. Sbarra^{23b}, A. Sbrizzi^{23a}, T. Scanlon⁹⁵, J. Schaarschmidt¹⁴⁹, P. Schacht¹¹⁵, B. M. Schachtner¹¹⁴, D. Schaefer³⁷, L. Schaefer¹³⁷, J. Schaeffer¹⁰⁰, S. Schaepe³⁶, U. Schäfer¹⁰⁰, A. C. Schaffer⁶⁵, D. Schaile¹¹⁴, R. D. Schamberger¹⁵⁶, N. Scharmberg¹⁰¹, V. A. Schegelsky¹³⁸, D. Scheirich¹⁴³, F. Schenck¹⁹, M. Schernau¹⁷², C. Schiavi^{55b,55a}, S. Schier¹⁴⁶, L. K. Schildgen²⁴, Z. M. Schillaci²⁶, E. J. Schioppa³⁶, M. Schioppa^{41b,41a}, K. E. Schleicher⁵², S. Schlenker³⁶, K. R. Schmidt-Sommerfeld¹¹⁵, K. Schmieden³⁶, C. Schmitt¹⁰⁰, S. Schmitt⁴⁶, S. Schmitz¹⁰⁰, J. C. Schmoeckel⁴⁶, U. Schnoor⁵², L. Schoeffel¹⁴⁵, A. Schoening^{61b}, P. G. Scholer⁵², E. Schopf¹³⁵, M. Schott¹⁰⁰, J. F. P. Schouwenberg¹¹⁹, J. Schovancova³⁶, S. Schramm⁵⁴, F. Schroeder¹⁸³, A. Schulte¹⁰⁰, H.-C. Schultz-Coulon^{61a}, M. Schumacher⁵², B. A. Schumm¹⁴⁶, Ph. Schune¹⁴⁵, A. Schwartzman¹⁵⁴, T. A. Schwarz¹⁰⁶, Ph. Schwemling¹⁴⁵, R. Schwienhorst¹⁰⁷, A. Sciandra¹⁴⁶, G. Sciolla²⁶, M. Scodreggio⁴⁶, M. Scornajenghi^{41b,41a}, F. Scuri^{72a}, F. Scutti¹⁰⁵, L. M. Scyboz¹¹⁵, C. D. Sebastiani^{73a,73b}, P. Seema¹⁹, S. C. Seidel¹¹⁸, A. Seiden¹⁴⁶, B. D. Seidlitz²⁹, T. Seiss³⁷, J. M. Seixas^{81b}, G. Sekhniaidze^{70a}, K. Sekhon¹⁰⁶, S. J. Sekula⁴², N. Semprini-Cesari^{23b,23a}, S. Sen⁴⁹, C. Serfon⁷⁷, L. Serin⁶⁵, L. Serkin^{67a,67b}, M. Sessa^{60a}, H. Severini¹²⁹, T. Šfiligoj⁹², F. Sforza^{55b,55a}, A. Sfyrila⁵⁴, E. Shabalina⁵³, J. D. Shahinian¹⁴⁶, N. W. Shaikh^{45a,45b}, D. Shaked Renous¹⁸¹, L. Y. Shan^{15a}, J. T. Shank²⁵, M. Shapiro¹⁸, A. Sharma¹³⁵, A. S. Sharma¹, P. B. Shatalov¹²⁴, K. Shaw¹⁵⁷, S. M. Shaw¹⁰¹, A. Shcherbakova¹³⁸, M. Shehade¹⁸¹,

Y. Shen¹²⁹, A. D. Sherman²⁵, P. Sherwood⁹⁵, L. Shi^{159,au}, S. Shimizu⁸², C. O. Shimmin¹⁸⁴, Y. Shimogama¹⁸⁰, M. Shimojima¹¹⁶, I. P. J. Shipsey¹³⁵, S. Shirabe⁸⁸, M. Shiyakova^{80,ad}, J. Shlomi¹⁸¹, A. Shmeleva¹¹¹, M. J. Shochet³⁷, J. Shojaii¹⁰⁵, D. R. Shope¹²⁹, S. Shrestha¹²⁷, E. M. Shrif^{33e}, E. Shulga¹⁸¹, P. Sicho¹⁴¹, A. M. Sickles¹⁷⁴, P. E. Sidebo¹⁵⁵, E. Sideras Haddad^{33e}, O. Sidiropoulou³⁶, A. Sidoti^{23b,23a}, F. Siegert⁴⁸, Dj. Sijacki¹⁶, M. Jr. Silva¹⁸², M. V. Silva Oliveira^{81a}, S. B. Silverstein^{45a}, S. Simion⁶⁵, E. Simioni¹⁰⁰, R. Simoniello¹⁰⁰, S. Simsek^{12b}, P. Sinervo¹⁶⁸, V. Sinetckii^{113,111}, N. B. Sinev¹³², M. Sioli^{23b,23a}, I. Siral¹⁰⁶, S. Yu. Sivoklokov¹¹³, J. Sjölin^{45a,45b}, E. Skorda⁹⁷, P. Skubic¹²⁹, M. Slawinska⁸⁵, K. Sliwa¹⁷¹, R. Slovak¹⁴³, V. Smakhtin¹⁸¹, B. H. Smart¹⁴⁴, J. Smiesko^{28a}, N. Smirnov¹¹², S. Yu. Smirnov¹¹², Y. Smirnov¹¹², L. N. Smirnova^{113,v}, O. Smirnova⁹⁷, J. W. Smith⁵³, M. Smizanska⁹⁰, K. Smolek¹⁴², A. Smykiewicz⁸⁵, A. A. Snesarev¹¹¹, H. L. Snoek¹²⁰, I. M. Snyder¹³², S. Snyder²⁹, R. Sobie^{177,af}, A. Soffer¹⁶², A. Søggaard⁵⁰, F. Sohns⁵³, C. A. Solans Sanchez³⁶, E. Yu. Soldatov¹¹², U. Soldevila¹⁷⁵, A. A. Solodkov¹²³, A. Soloshenko⁸⁰, O. V. Solovyanov¹²³, V. Solovyev¹³⁸, P. Sommer¹⁵⁰, H. Son¹⁷¹, W. Song¹⁴⁴, W. Y. Song^{169b}, A. Sopczak¹⁴², F. Sopkova^{28b}, C. L. Sotiropoulou^{72a,72b}, S. Sottocornola^{71a,71b}, R. Soualah^{67a,67c,g}, A. M. Soukharev^{122b,122a}, D. South⁴⁶, S. Spagnolo^{68a,68b}, M. Spalla¹¹⁵, M. Spangenberg¹⁷⁹, F. Spanò⁹⁴, D. Sperlich⁵², T. M. Spieker^{61a}, R. Spighi^{23b}, G. Spigo³⁶, M. Spina¹⁵⁷, D. P. Spiteri⁵⁷, M. Spousta¹⁴³, A. Stabile^{69a,69b}, B. L. Stamas¹²¹, R. Stamen^{61a}, M. Stamenkovic¹²⁰, E. Stanecka⁸⁵, B. Stanislaus¹³⁵, M. M. Stanitzki⁴⁶, M. Stankaityte¹³⁵, B. Stapf¹²⁰, E. A. Starchenko¹²³, G. H. Stark¹⁴⁶, J. Stark⁵⁸, S. H. Stark⁴⁰, P. Staroba¹⁴¹, P. Starovoitov^{61a}, S. Stärz¹⁰⁴, R. Staszewski⁸⁵, G. Stavropoulos⁴⁴, M. Stegler⁴⁶, P. Steinberg²⁹, A. L. Steinhebel¹³², B. Stelzer¹⁵³, H. J. Stelzer¹³⁹, O. Stelzer-Chilton^{169a}, H. Stenzel⁵⁶, T. J. Stevenson¹⁵⁷, G. A. Stewart³⁶, M. C. Stockton³⁶, G. Stoica^{27b}, M. Stolarski^{140a}, S. Stonjek¹¹⁵, A. Straessner⁴⁸, J. Strandberg¹⁵⁵, S. Strandberg^{45a,45b}, M. Strauss¹²⁹, P. Strizenec^{28b}, R. Ströhmer¹⁷⁸, D. M. Strom¹³², R. Stroynowski⁴², A. Strubig⁵⁰, S. A. Stucci²⁹, B. Stugu¹⁷, J. Stupak¹²⁹, N. A. Styles⁴⁶, D. Su¹⁵⁴, S. Suchek^{61a}, V. V. Sulin¹¹¹, M. J. Sullivan⁹¹, D. M. S. Sultan⁵⁴, S. Sultansoy^{4c}, T. Sumida⁸⁶, S. Sun¹⁰⁶, X. Sun³, K. Suruliz¹⁵⁷, C. J. E. Suster¹⁵⁸, M. R. Sutton¹⁵⁷, S. Suzuki⁸², M. Svatos¹⁴¹, M. Swiatlowski³⁷, S. P. Swift², T. Swirski¹⁷⁸, A. Sydorenko¹⁰⁰, I. Sykora^{28a}, M. Sykora¹⁴³, T. Sykora¹⁴³, D. Ta¹⁰⁰, K. Tackmann^{46,ab}, J. Taenzer¹⁶², A. Taffard¹⁷², R. Tafirout^{169a}, H. Takai²⁹, R. Takashima⁸⁷, K. Takeda⁸³, T. Takeshita¹⁵¹, E. P. Takeva⁵⁰, Y. Takubo⁸², M. Talby¹⁰², A. A. Talyshev^{122b,122a}, N. M. Tamir¹⁶², J. Tanaka¹⁶⁴, M. Tanaka¹⁶⁶, R. Tanaka⁶⁵, S. Tapia Araya¹⁷⁴, S. Tapprogge¹⁰⁰, A. Tarek Abouelfadl Mohamed¹³⁶, S. Tarem¹⁶¹, K. Tariq^{60b}, G. Tarna^{27b,c}, G. F. Tartarelli^{69a}, P. Tas¹⁴³, M. Tasevsky¹⁴¹, T. Tashiro⁸⁶, E. Tassi^{41b,41a}, A. Tavares Delgado^{140a,140b}, Y. Tayalati^{35c}, A. J. Taylor⁵⁰, G. N. Taylor¹⁰⁵, W. Taylor^{169b}, A. S. Tee⁹⁰, R. Teixeira De Lima¹⁵⁴, P. Teixeira-Dias⁹⁴, H. Ten Kate³⁶, J. J. Teoh¹²⁰, S. Terada⁸², K. Terashi¹⁶⁴, J. Terron⁹⁹, S. Terzo¹⁴, M. Testa⁵¹, R. J. Teuscher^{168,af}, S. J. Thais¹⁸⁴, T. Thevenaux-Pelzer⁴⁶, F. Thiele⁴⁰, D. W. Thomas⁹⁴, J. O. Thomas⁴², J. P. Thomas²¹, A. S. Thompson⁵⁷, P. D. Thompson²¹, L. A. Thomsen¹⁸⁴, E. Thomson¹³⁷, E. J. Thorpe⁹³, R. E. Ticse Torres⁵³, V. O. Tikhomirov^{111,aq}, Yu. A. Tikhonov^{122b,122a}, S. Timoshenko¹¹², P. Tipton¹⁸⁴, S. Tisserant¹⁰², K. Todome^{23b,23a}, S. Todorova-Nova⁵, S. Todt⁴⁸, J. Tojo⁸⁸, S. Tokár^{28a}, K. Tokushuku⁸², E. Tolley¹²⁷, K. G. Tomiwa^{33e}, M. Tomoto¹¹⁷, L. Tompkins^{154,q}, B. Tong⁵⁹, P. Tornambe¹⁰³, E. Torrence¹³², H. Torres⁴⁸, E. Torró Pastor¹⁴⁹, C. Toscirri¹³⁵, J. Toth^{102,ae}, D. R. Tovey¹⁵⁰, A. Traeet¹⁷, C. J. Treado¹²⁵, T. Trefzger¹⁷⁸, F. Tresoldi¹⁵⁷, A. Tricoli²⁹, I. M. Trigger^{169a}, S. Trincaz-Duvoid¹³⁶, D. A. Trischuk¹⁷⁶, W. Trischuk¹⁶⁸, B. Trocmé⁵⁸, A. Trofymov¹⁴⁵, C. Troncon^{69a}, M. Trovattelli¹⁷⁷, F. Trovato¹⁵⁷, L. Truong^{33c}, M. Trzebinski⁸⁵, A. Trzupek⁸⁵, F. Tsai⁴⁶, J.C.-L. Tseng¹³⁵, P. V. Tsiareshka^{108,al}, A. Tsirigotis^{163,y}, V. Tsiskaridze¹⁵⁶, E. G. Tskhadadze^{160a}, M. Tsopoulou¹⁶³, I. I. Tsukerman¹²⁴, V. Tsulaia¹⁸, S. Tsuno⁸², D. Tsybychev¹⁵⁶, Y. Tu^{63b}, A. Tudorache^{27b}, V. Tudorache^{27b}, T. T. Tulbure^{27a}, A. N. Tuna⁵⁹, S. Turchikhin⁸⁰, D. Turgeman¹⁸¹, I. Turk Cakir^{4b,w}, R. J. Turner²¹, R. Turra^{69a}, P. M. Tuts³⁹, S. Tzamarias¹⁶³, E. Tzovara¹⁰⁰, G. Uchielli⁴⁷, K. Uchida¹⁶⁴, I. Ueda⁸², M. Ughetto^{45a,45b}, F. Ukegawa¹⁷⁰, G. Unal³⁶, A. Undrus²⁹, G. Unel¹⁷², F. C. Ungaro¹⁰⁵, Y. Unno⁸², K. Uno¹⁶⁴, J. Urban^{28b}, P. Urquijo¹⁰⁵, G. Usai⁸, Z. Uysal^{12d}, V. Vacek¹⁴², B. Vachon¹⁰⁴, K. O. H. Vadla¹³⁴, A. Vaidya⁹⁵, C. Valderanis¹¹⁴, E. Valdes Santurio^{45a,45b}, M. Valente⁵⁴, S. Valentinetti^{23b,23a}, A. Valero¹⁷⁵, L. Valéry⁴⁶, R. A. Vallance²¹, A. Vallier³⁶, J. A. Valls Ferrer¹⁷⁵, T. R. Van Daalen¹⁴, P. Van Gemmeren⁶, I. Van Vulpen¹²⁰, M. Vanadia^{74a,74b}, W. Vandelli³⁶, E. R. Vandewall¹³⁰, A. Vaniachine¹⁶⁷, D. Vannicola^{73a,73b}, R. Vari^{73a}, E. W. Varnes⁷, C. Varni^{55b,55a}, T. Varol¹⁵⁹, D. Varouchas⁶⁵, K. E. Varvell¹⁵⁸, M. E. Vasile^{27b}, G. A. Vasquez¹⁷⁷, J. G. Vasquez¹⁸⁴, F. Vazeille³⁸, D. Vazquez Furelos¹⁴, T. Vazquez Schroeder³⁶, J. Veatch⁵³, V. Vecchio^{75a,75b}, M. J. Veen¹²⁰, L. M. Veloce¹⁶⁸, F. Veloso^{140a,140c}, S. Veneziano^{73a}, A. Ventura^{68a,68b}, N. Venturi³⁶, A. Verbitskyi¹¹⁵

V. Vercesi^{71a}, M. Verducci^{72a,72b}, C. M. Vergel Infante⁷⁹, C. Vergis²⁴, W. Verkerke¹²⁰, A. T. Vermeulen¹²⁰, J. C. Vermeulen¹²⁰, M. C. Vetterli^{153,ax}, N. Viaux Maira^{147d}, M. Vicente Barreto Pinto⁵⁴, T. Vickey¹⁵⁰, O. E. Vickey Boeriu¹⁵⁰, G. H. A. Viehhauser¹³⁵, L. Vigani^{61b}, M. Villa^{23b,23a}, M. Villaplana Perez^{69a,69b}, E. Vilucchi⁵¹, M. G. Vincter³⁴, G. S. Virdee²¹, A. Vishwakarma⁴⁶, C. Vittori^{23b,23a}, I. Vivarelli¹⁵⁷, M. Vogel¹⁸³, P. Vokac¹⁴², S. E. von Buddenbrock^{33c}, E. Von Toerne²⁴, V. Vorobel¹⁴³, K. Vorobev¹¹², M. Vos¹⁷⁵, J. H. Vosseveld⁹¹, M. Vozak¹⁰¹, N. Vranjes¹⁶, M. Vranjes Milosavljevic¹⁶, V. Vrba¹⁴², M. Vreeswijk¹²⁰, R. Vuillermet³⁶, I. Vukotic³⁷, P. Wagner²⁴, W. Wagner¹⁸³, J. Wagner-Kuhr¹¹⁴, S. Wahdan¹⁸³, H. Wahlberg⁸⁹, V. M. Walbrecht¹¹⁵, J. Walder⁹⁰, R. Walker¹¹⁴, S. D. Walker⁹⁴, W. Walkowiak¹⁵², V. Wallangen^{45a,45b}, A. M. Wang⁵⁹, C. Wang^{60c}, C. Wang^{60b}, F. Wang¹⁸², H. Wang¹⁸, H. Wang³, J. Wang^{63a}, J. Wang¹⁵⁸, J. Wang^{61b}, P. Wang⁴², Q. Wang¹²⁹, R.-J. Wang¹⁰⁰, R. Wang^{60a}, R. Wang⁶, S. M. Wang¹⁵⁹, W. T. Wang^{60a}, W. Wang^{15c,ag}, W. X. Wang^{60a,ag}, Y. Wang^{60a,an}, Z. Wang^{60c}, C. Wanotayaroj⁴⁶, A. Warburton¹⁰⁴, C. P. Ward³², D. R. Wardrope⁹⁵, N. Warrack⁵⁷, A. Washbrook⁵⁰, A. T. Watson²¹, M. F. Watson²¹, G. Watts¹⁴⁹, B. M. Waugh⁹⁵, A. F. Webb¹¹, S. Webb¹⁰⁰, C. Weber¹⁸⁴, M. S. Weber²⁰, S. A. Weber³⁴, S. M. Weber^{61a}, A. R. Weidberg¹³⁵, J. Weingarten⁴⁷, M. Weirich¹⁰⁰, C. Weiser⁵², P. S. Wells³⁶, T. Wenaus²⁹, T. Wengler³⁶, S. Wenig³⁶, N. Wermes²⁴, M. D. Werner⁷⁹, M. Wessels^{61a}, T. D. Weston²⁰, K. Whalen¹³², N. L. Whallon¹⁴⁹, A. M. Wharton⁹⁰, A. S. White¹⁰⁶, A. White⁸, M. J. White¹, D. Whiteson¹⁷², B. W. Whitmore⁹⁰, W. Wiedenmann¹⁸², M. Wielers¹⁴⁴, N. Wieseotte¹⁰⁰, C. Wiglesworth⁴⁰, L. A. M. Wiik-Fuchs⁵², F. Wilk¹⁰¹, H. G. Wilkens³⁶, L. J. Wilkins⁹⁴, H. H. Williams¹³⁷, S. Williams³², C. Willis¹⁰⁷, S. Willocq¹⁰³, J. A. Wilson²¹, I. Wingerter-Seez⁵, E. Winkels¹⁵⁷, F. Winklmeier¹³², O. J. Winston¹⁵⁷, B. T. Winter⁵², M. Wittgen¹⁵⁴, M. Wobisch⁹⁶, A. Wolf¹⁰⁰, T. M. H. Wolf¹²⁰, R. Wolff¹⁰², R. Wölker¹³⁵, J. Wollrath⁵², M. W. Wolter⁸⁵, H. Wolters^{140a,140c}, V. W. S. Wong¹⁷⁶, N. L. Woods¹⁴⁶, S. D. Worm²¹, B. K. Wosiek⁸⁵, K. W. Woźniak⁸⁵, K. Wraight⁵⁷, S. L. Wu¹⁸², X. Wu⁵⁴, Y. Wu^{60a}, T. R. Wyatt¹⁰¹, B. M. Wynne⁵⁰, S. Xella⁴⁰, Z. Xi¹⁰⁶, L. Xia¹⁷⁹, X. Xiao¹⁰⁶, I. Xiotidis¹⁵⁷, D. Xu^{15a}, H. Xu^{60a,c}, L. Xu²⁹, T. Xu¹⁴⁵, W. Xu¹⁰⁶, Z. Xu^{60b}, Z. Xu¹⁵⁴, B. Yabsley¹⁵⁸, S. Yacoub^{33a}, K. Yajima¹³³, D. P. Yallup⁹⁵, D. Yamaguchi¹⁶⁶, Y. Yamaguchi¹⁶⁶, A. Yamamoto⁸², M. Yamatani¹⁶⁴, T. Yamazaki¹⁶⁴, Y. Yamazaki⁸³, Z. Yan²⁵, H. J. Yang^{60c,60d}, H. T. Yang¹⁸, S. Yang⁷⁸, X. Yang^{60b,58}, Y. Yang¹⁶⁴, W.-M. Yao¹⁸, Y. C. Yap⁴⁶, Y. Yasu⁸², E. Yatsenko^{60c,60d}, J. Ye⁴², S. Ye²⁹, I. Yeletsikhik⁸⁰, M. R. Yexley⁹⁰, E. Yigitbasi²⁵, K. Yorita¹⁸⁰, K. Yoshihara¹³⁷, C. J. S. Young³⁶, C. Young¹⁵⁴, J. Yu⁷⁹, R. Yuan^{60b,i}, X. Yue^{61a}, S. P. Y. Yuen²⁴, M. Zaazoua^{35c}, B. Zabinski⁸⁵, G. Zacharis¹⁰, E. Zaffaroni⁵⁴, J. Zahreddine¹³⁶, A. M. Zaitsev^{123,ap}, T. Zakareishvili^{160b}, N. Zakharchuk³⁴, S. Zambito⁵⁹, D. Zanzi³⁶, D. R. Zaripovas⁵⁷, S. V. Zeiβner⁴⁷, C. Zeitnitz¹⁸³, G. Zemaityte¹³⁵, J. C. Zeng¹⁷⁴, O. Zenin¹²³, T. Ženiš^{28a}, D. Zerwas⁶⁵, M. Zgubič¹³⁵, B. Zhang^{15c}, D. F. Zhang^{15b}, G. Zhang^{15b}, H. Zhang^{15c}, J. Zhang⁶, L. Zhang^{15c}, L. Zhang^{60a}, M. Zhang¹⁷⁴, R. Zhang²⁴, X. Zhang^{60b}, Y. Zhang^{15a,15d}, Z. Zhang^{63a}, Z. Zhang⁶⁵, P. Zhao⁴⁹, Y. Zhao^{60b}, Z. Zhao^{60a}, A. Zhemchugov⁸⁰, Z. Zheng¹⁰⁶, D. Zhong¹⁷⁴, B. Zhou¹⁰⁶, C. Zhou¹⁸², M. S. Zhou^{15a,15d}, M. Zhou¹⁵⁶, N. Zhou^{60c}, Y. Zhou⁷, C. G. Zhu^{60b}, C. Zhu^{15a,15d}, H. L. Zhu^{60a}, H. Zhu^{15a}, J. Zhu¹⁰⁶, Y. Zhu^{60a}, X. Zhuang^{15a}, K. Zhukov¹¹¹, V. Zhulanov^{122b,122a}, D. Zieminska⁶⁶, N. I. Zimine⁸⁰, S. Zimmermann^{52,*}, Z. Zinonos¹¹⁵, M. Ziolkowski¹⁵², L. Živković¹⁶, G. Zobernig¹⁸², A. Zoccoli^{23b,23a}, K. Zoch⁵³, T. G. Zorbas¹⁵⁰, R. Zou³⁷, L. Zwalinski³⁶

¹ Department of Physics, University of Adelaide, Adelaide, Australia

² Physics Department, SUNY Albany, Albany, NY, USA

³ Department of Physics, University of Alberta, Edmonton, AB, Canada

⁴ (a)Department of Physics, Ankara University, Ankara, Turkey; (b)Application and Research Center for Advanced Studies, Istanbul Aydin University, Istanbul, Turkey; (c)Division of Physics, TOBB University of Economics and Technology, Ankara, Turkey

⁵ LAPP, Université Grenoble Alpes, Université Savoie Mont Blanc, CNRS/IN2P3, Annecy, France

⁶ High Energy Physics Division, Argonne National Laboratory, Argonne, IL, USA

⁷ Department of Physics, University of Arizona, Tucson, AZ, USA

⁸ Department of Physics, University of Texas at Arlington, Arlington, TX, USA

⁹ Physics Department, National and Kapodistrian University of Athens, Athens, Greece

¹⁰ Physics Department, National Technical University of Athens, Zografou, Greece

¹¹ Department of Physics, University of Texas at Austin, Austin, TX, USA

- ¹² (a) Bahcesehir University, Faculty of Engineering and Natural Sciences, Istanbul, Turkey; (b) Istanbul Bilgi University, Faculty of Engineering and Natural Sciences, Istanbul, Turkey; (c) Department of Physics, Bogazici University, Istanbul, Turkey; (d) Department of Physics Engineering, Gaziantep University, Gaziantep, Turkey
- ¹³ Institute of Physics, Azerbaijan Academy of Sciences, Baku, Azerbaijan
- ¹⁴ Institut de Física d'Altes Energies (IFAE), Barcelona Institute of Science and Technology, Barcelona, Spain
- ¹⁵ (a) Institute of High Energy Physics, Chinese Academy of Sciences, Beijing, China; (b) Physics Department, Tsinghua University, Beijing, China; (c) Department of Physics, Nanjing University, Nanjing, China; (d) University of Chinese Academy of Science (UCAS), Beijing, China
- ¹⁶ Institute of Physics, University of Belgrade, Belgrade, Serbia
- ¹⁷ Department for Physics and Technology, University of Bergen, Bergen, Norway
- ¹⁸ Physics Division, Lawrence Berkeley National Laboratory and University of California, Berkeley, CA, USA
- ¹⁹ Institut für Physik, Humboldt Universität zu Berlin, Berlin, Germany
- ²⁰ Albert Einstein Center for Fundamental Physics and Laboratory for High Energy Physics, University of Bern, Bern, Switzerland
- ²¹ School of Physics and Astronomy, University of Birmingham, Birmingham, UK
- ²² (a) Facultad de Ciencias y Centro de Investigaciones, Universidad Antonio Nariño, Bogotá, Colombia; (b) Departamento de Física, Universidad Nacional de Colombia, Bogotá, Colombia, Colombia
- ²³ (a) Dipartimento di Fisica, INFN Bologna and Università di Bologna, Bologna, Italy; (b) INFN Sezione di Bologna, Bologna, Italy
- ²⁴ Physikalisches Institut, Universität Bonn, Bonn, Germany
- ²⁵ Department of Physics, Boston University, Boston, MA, USA
- ²⁶ Department of Physics, Brandeis University, Waltham, MA, USA
- ²⁷ (a) Transilvania University of Brasov, Brasov, Romania; (b) Horia Hulubei National Institute of Physics and Nuclear Engineering, Bucharest, Romania; (c) Department of Physics, Alexandru Ioan Cuza University of Iasi, Iasi, Romania; (d) National Institute for Research and Development of Isotopic and Molecular Technologies, Physics Department, Cluj-Napoc, Romania; (e) University Politehnica Bucharest, Bucharest, Romania; (f) West University in Timisoara, Timisoara, Romania
- ²⁸ (a) Faculty of Mathematics, Physics and Informatics, Comenius University, Bratislava, Slovak Republic; (b) Department of Subnuclear Physics, Institute of Experimental Physics of the Slovak Academy of Sciences, Kosice, Slovak Republic
- ²⁹ Physics Department, Brookhaven National Laboratory, Upton, NY, USA
- ³⁰ Departamento de Física, Universidad de Buenos Aires, Buenos Aires, Argentina
- ³¹ California State University, Long Beach, CA, USA
- ³² Cavendish Laboratory, University of Cambridge, Cambridge, UK
- ³³ (a) Department of Physics, University of Cape Town, Cape Town, South Africa; (b) iThemba Labs, Western Cape, South Africa; (c) Department of Mechanical Engineering Science, University of Johannesburg, Johannesburg, South Africa; (d) University of South Africa, Department of Physics, Pretoria, South Africa; (e) School of Physics, University of the Witwatersrand, Johannesburg, South Africa
- ³⁴ Department of Physics, Carleton University, Ottawa, ON, Canada
- ³⁵ (a) Faculté des Sciences Ain Chock, Réseau Universitaire de Physique des Hautes Energies - Université Hassan II, Casablanca, Morocco; (b) Faculté des Sciences, Université Ibn-Tofail, Kénitra, Morocco; (c) Faculté des Sciences Semlalia, Université Cadi Ayyad, LPHEA-Marrakech, Marrakech, Morocco; (d) Faculté des Sciences, Université Mohamed Premier and LPTPM, Oujda, Switzerland; (e) Faculté des sciences, Université Mohammed V, Rabat, Morocco
- ³⁶ CERN, Geneva, Switzerland
- ³⁷ Enrico Fermi Institute, University of Chicago, Chicago, IL, USA
- ³⁸ LPC, Université Clermont Auvergne, CNRS/IN2P3, Clermont-Ferrand, France
- ³⁹ Nevis Laboratory, Columbia University, Irvington, NY, USA
- ⁴⁰ Niels Bohr Institute, University of Copenhagen, Copenhagen, Denmark
- ⁴¹ (a) Dipartimento di Fisica, Università della Calabria, Rende, Italy; (b) INFN Gruppo Collegato di Cosenza, Laboratori Nazionali di Frascati, Frascati, Italy
- ⁴² Physics Department, Southern Methodist University, Dallas, TX, USA
- ⁴³ Physics Department, University of Texas at Dallas, Richardson, TX, USA
- ⁴⁴ National Centre for Scientific Research "Demokritos", Agia Paraskevi, Greece
- ⁴⁵ (a) Department of Physics, Stockholm University, Stockholm, Sweden; (b) Oskar Klein Centre, Stockholm, Sweden

- ⁴⁶ Deutsches Elektronen-Synchrotron DESY, Hamburg and Zeuthen, Germany
- ⁴⁷ Lehrstuhl für Experimentelle Physik IV, Technische Universität Dortmund, Dortmund, Germany
- ⁴⁸ Institut für Kern- und Teilchenphysik, Technische Universität Dresden, Dresden, Germany
- ⁴⁹ Department of Physics, Duke University, Durham, NC, USA
- ⁵⁰ SUPA, School of Physics and Astronomy, University of Edinburgh, Edinburgh, UK
- ⁵¹ INFN e Laboratori Nazionali di Frascati, Frascati, Italy
- ⁵² Physikalisches Institut, Albert-Ludwigs-Universität Freiburg, Freiburg, Germany
- ⁵³ II. Physikalisches Institut, Georg-August-Universität Göttingen, Göttingen, Germany
- ⁵⁴ Département de Physique Nucléaire et Corpusculaire, Université de Genève, Geneva, Switzerland
- ⁵⁵ ^(a)Dipartimento di Fisica, Università di Genova, Genoa, Italy; ^(b)INFN Sezione di Genova, Genoa, Italy
- ⁵⁶ II. Physikalisches Institut, Justus-Liebig-Universität Giessen, Giessen, Germany
- ⁵⁷ SUPA, School of Physics and Astronomy, University of Glasgow, Glasgow, UK
- ⁵⁸ LPSC, Université Grenoble Alpes, CNRS/IN2P3, Grenoble INP, Grenoble, France
- ⁵⁹ Laboratory for Particle Physics and Cosmology, Harvard University, Cambridge, MA, USA
- ⁶⁰ ^(a)Department of Modern Physics and State Key Laboratory of Particle Detection and Electronics, University of Science and Technology of China, Hefei, China; ^(b)Institute of Frontier and Interdisciplinary Science and Key Laboratory of Particle Physics and Particle Irradiation (MOE), Shandong University, Qingdao, China; ^(c)School of Physics and Astronomy, Shanghai Jiao Tong University, KLPPAC-MoE, SKLPPC, Shanghai, China; ^(d)Tsung-Dao Lee Institute, Shanghai, China
- ⁶¹ ^(a)Kirchhoff-Institut für Physik, Ruprecht-Karls-Universität Heidelberg, Heidelberg, Germany; ^(b)Physikalisches Institut, Ruprecht-Karls-Universität Heidelberg, Heidelberg, Germany
- ⁶² Faculty of Applied Information Science, Hiroshima Institute of Technology, Hiroshima, Japan
- ⁶³ ^(a)Department of Physics, Chinese University of Hong Kong, Shatin, N.T., Hong Kong, China; ^(b)Department of Physics, University of Hong Kong, Hong Kong, China; ^(c)Department of Physics and Institute for Advanced Study, Hong Kong University of Science and Technology, Clear Water Bay, Kowloon, Hong Kong, China
- ⁶⁴ Department of Physics, National Tsing Hua University, Hsinchu, Taiwan
- ⁶⁵ IJCLab, Université Paris-Saclay, CNRS/IN2P3, 91405, Orsay, France
- ⁶⁶ Department of Physics, Indiana University, Bloomington, IN, USA
- ⁶⁷ ^(a)INFN Gruppo Collegato di Udine, Sezione di Trieste, Udine, Italy; ^(b)ICTP, Trieste, Italy; ^(c)Dipartimento Politecnico di Ingegneria e Architettura, Università di Udine, Udine, Italy
- ⁶⁸ ^(a)INFN Sezione di Lecce, Lecce, Italy; ^(b)Dipartimento di Matematica e Fisica, Università del Salento, Lecce, Italy
- ⁶⁹ ^(a)INFN Sezione di Milano, Milan, Italy; ^(b)Dipartimento di Fisica, Università di Milano, Milan, Italy
- ⁷⁰ ^(a)INFN Sezione di Napoli, Naples, Italy; ^(b)Dipartimento di Fisica, Università di Napoli, Naples, Italy
- ⁷¹ ^(a)INFN Sezione di Pavia, Pavia, Italy; ^(b)Dipartimento di Fisica, Università di Pavia, Pavia, Italy
- ⁷² ^(a)INFN Sezione di Pisa, Pisa, Italy; ^(b)Dipartimento di Fisica E. Fermi, Università di Pisa, Pisa, Italy
- ⁷³ ^(a)INFN Sezione di Roma, Rome, Italy; ^(b)Dipartimento di Fisica, Sapienza Università di Roma, Rome, Italy
- ⁷⁴ ^(a)INFN Sezione di Roma Tor Vergata, Rome, Italy; ^(b)Dipartimento di Fisica, Università di Roma Tor Vergata, Rome, Italy
- ⁷⁵ ^(a)INFN Sezione di Roma Tre, Rome, Italy; ^(b)Dipartimento di Matematica e Fisica, Università Roma Tre, Rome, Italy
- ⁷⁶ ^(a)INFN-TIFPA, Trento, Italy; ^(b)Università degli Studi di Trento, Trento, Italy
- ⁷⁷ Institut für Astro- und Teilchenphysik, Leopold-Franzens-Universität, Innsbruck, Austria
- ⁷⁸ University of Iowa, Iowa City, IA, USA
- ⁷⁹ Department of Physics and Astronomy, Iowa State University, Ames, IA, USA
- ⁸⁰ Joint Institute for Nuclear Research, Dubna, Russia
- ⁸¹ ^(a)Departamento de Engenharia Elétrica, Universidade Federal de Juiz de Fora (UFJF), Juiz de Fora, Brazil ; ^(b)Universidade Federal do Rio De Janeiro COPPE/EE/IF, Rio de Janeiro, Brazil; ^(c)Instituto de Física, Universidade de São Paulo, São Paulo, Brazil
- ⁸² KEK, High Energy Accelerator Research Organization, Tsukuba, Japan
- ⁸³ Graduate School of Science, Kobe University, Kobe, Japan
- ⁸⁴ ^(a)AGH University of Science and Technology, Faculty of Physics and Applied Computer Science, Kraków, Poland ; ^(b)Marian Smoluchowski Institute of Physics, Jagiellonian University, Kraków, Poland
- ⁸⁵ Institute of Nuclear Physics Polish Academy of Sciences, Kraków, Poland
- ⁸⁶ Faculty of Science, Kyoto University, Kyoto, Japan

- 87 Kyoto University of Education, Kyoto, Japan
- 88 Research Center for Advanced Particle Physics and Department of Physics, Kyushu University, Fukuoka, Japan
- 89 Instituto de Física La Plata, Universidad Nacional de La Plata and CONICET, La Plata, Argentina
- 90 Physics Department, Lancaster University, Lancaster, UK
- 91 Oliver Lodge Laboratory, University of Liverpool, Liverpool, UK
- 92 Department of Experimental Particle Physics, Jožef Stefan Institute and Department of Physics, University of Ljubljana, Ljubljana, Slovenia
- 93 School of Physics and Astronomy, Queen Mary University of London, London, UK
- 94 Department of Physics, Royal Holloway University of London, Egham, UK
- 95 Department of Physics and Astronomy, University College London, London, UK
- 96 Louisiana Tech University, Ruston, LA, USA
- 97 Fysiska institutionen, Lunds universitet, Lund, Sweden
- 98 Centre de Calcul de l'Institut National de Physique Nucléaire et de Physique des Particules (IN2P3), Villeurbanne, France
- 99 Departamento de Física Teórica C-15 and CIAFF, Universidad Autónoma de Madrid, Madrid, Spain
- 100 Institut für Physik, Universität Mainz, Mainz, Germany
- 101 School of Physics and Astronomy, University of Manchester, Manchester, UK
- 102 CPPM, Aix-Marseille Université, CNRS/IN2P3, Marseille, France
- 103 Department of Physics, University of Massachusetts, Amherst, MA, USA
- 104 Department of Physics, McGill University, Montreal, QC, Canada
- 105 School of Physics, University of Melbourne, Melbourne VIC, Australia
- 106 Department of Physics, University of Michigan, Ann Arbor, MI, USA
- 107 Department of Physics and Astronomy, Michigan State University, East Lansing, MI, USA
- 108 B.I. Stepanov Institute of Physics, National Academy of Sciences of Belarus, Minsk, Belarus
- 109 Research Institute for Nuclear Problems of Byelorussian State University, Minsk, Belarus
- 110 Group of Particle Physics, University of Montreal, Montreal, QC, Canada
- 111 P.N. Lebedev Physical Institute of the Russian Academy of Sciences, Moscow, Russia
- 112 National Research Nuclear University MEPhI, Moscow, Russia
- 113 D.V. Skobeltsyn Institute of Nuclear Physics, M.V. Lomonosov Moscow State University, Moscow, Russia
- 114 Fakultät für Physik, Ludwig-Maximilians-Universität München, Munich, Germany
- 115 Max-Planck-Institut für Physik (Werner-Heisenberg-Institut), Munich, Germany
- 116 Nagasaki Institute of Applied Science, Nagasaki, Japan
- 117 Graduate School of Science and Kobayashi-Maskawa Institute, Nagoya University, Nagoya, Japan
- 118 Department of Physics and Astronomy, University of New Mexico, Albuquerque, NM, USA
- 119 Institute for Mathematics, Astrophysics and Particle Physics, Radboud University Nijmegen/Nikhef, Nijmegen, The Netherlands
- 120 Nikhef National Institute for Subatomic Physics and University of Amsterdam, Amsterdam, The Netherlands
- 121 Department of Physics, Northern Illinois University, DeKalb, IL, USA
- 122 (a) Budker Institute of Nuclear Physics and NSU, SB RAS, Novosibirsk, Russia; (b) Novosibirsk State University Novosibirsk, Novosibirsk, Russia
- 123 Institute for High Energy Physics of the National Research Centre Kurchatov Institute, Protvino, Russia
- 124 Institute for Theoretical and Experimental Physics named by A.I. Alikhanov of National Research Centre "Kurchatov Institute", Moscow, Russia
- 125 Department of Physics, New York University, New York, NY, USA
- 126 Ochanomizu University, Otsuka, Bunkyo-ku, Tokyo, Japan
- 127 Ohio State University, Columbus, OH, USA
- 128 Faculty of Science, Okayama University, Okayama, Japan
- 129 Homer L. Dodge Department of Physics and Astronomy, University of Oklahoma, Norman, OK, USA
- 130 Department of Physics, Oklahoma State University, Stillwater, OK, USA
- 131 Palacký University, RCPTM, Joint Laboratory of Optics, Olomouc, Czech Republic
- 132 Institute for Fundamental Science, University of Oregon, Eugene, OR, USA
- 133 Graduate School of Science, Osaka University, Osaka, Japan
- 134 Department of Physics, University of Oslo, Oslo, Norway

- 135 Department of Physics, Oxford University, Oxford, UK
- 136 LPNHE, Sorbonne Université, Université de Paris, CNRS/IN2P3, Paris, France
- 137 Department of Physics, University of Pennsylvania, Philadelphia, PA, USA
- 138 Konstantinov Nuclear Physics Institute of National Research Centre “Kurchatov Institute”, PNPI, St. Petersburg, Russia
- 139 Department of Physics and Astronomy, University of Pittsburgh, Pittsburgh, PA, USA
- 140 ^(a)Laboratório de Instrumentação e Física Experimental de Partículas - LIP, Lisbon, Portugal; ^(b)Departamento de Física, Faculdade de Ciências, Universidade de Lisboa, Lisbon, Portugal; ^(c)Departamento de Física, Universidade de Coimbra, Coimbra, Portugal; ^(d)Centro de Física Nuclear da Universidade de Lisboa, Lisbon, Portugal; ^(e)Departamento de Física, Universidade do Minho, Braga, Portugal; ^(f)Departamento de Física Teórica y del Cosmos, Universidad de Granada, Granada, Spain; ^(g)Dep Física and CEFITEC of Faculdade de Ciências e Tecnologia, Universidade Nova de Lisboa, Caparica, Portugal; ^(h)Instituto Superior Técnico, Universidade de Lisboa, Lisbon, Portugal
- 141 Institute of Physics of the Czech Academy of Sciences, Prague, Czech Republic
- 142 Czech Technical University in Prague, Prague, Czech Republic
- 143 Charles University, Faculty of Mathematics and Physics, Prague, Czech Republic
- 144 Particle Physics Department, Rutherford Appleton Laboratory, Didcot, UK
- 145 IRFU, CEA, Université Paris-Saclay, Gif-sur-Yvette, France
- 146 Santa Cruz Institute for Particle Physics, University of California Santa Cruz, Santa Cruz, CA, USA
- 147 ^(a)Departamento de Física, Pontificia Universidad Católica de Chile, Santiago, Chile; ^(b)Universidad Andres Bello, Department of Physics, Santiago, Chile; ^(c)Instituto de Alta Investigación, Universidad de Tarapacá, Santiago, Chile; ^(d)Departamento de Física, Universidad Técnica Federico Santa María, Valparaíso, Chile
- 148 Universidade Federal de São João del Rei (UFSJ), São João del Rei, Brazil
- 149 Department of Physics, University of Washington, Seattle, WA, USA
- 150 Department of Physics and Astronomy, University of Sheffield, Sheffield, UK
- 151 Department of Physics, Shinshu University, Nagano, Japan
- 152 Department Physik, Universität Siegen, Siegen, Germany
- 153 Department of Physics, Simon Fraser University, Burnaby, BC, Canada
- 154 SLAC National Accelerator Laboratory, Stanford, CA, USA
- 155 Physics Department, Royal Institute of Technology, Stockholm, Sweden
- 156 Departments of Physics and Astronomy, Stony Brook University, Stony Brook, NY, USA
- 157 Department of Physics and Astronomy, University of Sussex, Brighton, UK
- 158 School of Physics, University of Sydney, Sydney, Australia
- 159 Institute of Physics, Academia Sinica, Taipei, Taiwan
- 160 ^(a)E. Andronikashvili Institute of Physics, Iv. Javakhishvili Tbilisi State University, Tbilisi, Georgia; ^(b)High Energy Physics Institute, Tbilisi State University, Tbilisi, Georgia
- 161 Department of Physics, Technion, Israel Institute of Technology, Haifa, Israel
- 162 Raymond and Beverly Sackler School of Physics and Astronomy, Tel Aviv University, Tel Aviv, Israel
- 163 Department of Physics, Aristotle University of Thessaloniki, Thessaloniki, Greece
- 164 International Center for Elementary Particle Physics and Department of Physics, University of Tokyo, Tokyo, Japan
- 165 Graduate School of Science and Technology, Tokyo Metropolitan University, Tokyo, Japan
- 166 Department of Physics, Tokyo Institute of Technology, Tokyo, Japan
- 167 Tomsk State University, Tomsk, Russia
- 168 Department of Physics, University of Toronto, Toronto, ON, Canada
- 169 ^(a)TRIUMF, Vancouver, BC, Canada; ^(b)Department of Physics and Astronomy, York University, Toronto, ON, Canada
- 170 Division of Physics and Tomonaga Center for the History of the Universe, Faculty of Pure and Applied Sciences, University of Tsukuba, Tsukuba, Japan
- 171 Department of Physics and Astronomy, Tufts University, Medford, MA, USA
- 172 Department of Physics and Astronomy, University of California Irvine, Irvine, CA, USA
- 173 Department of Physics and Astronomy, University of Uppsala, Uppsala, Sweden
- 174 Department of Physics, University of Illinois, Urbana, IL, USA
- 175 Instituto de Física Corpuscular (IFIC), Centro Mixto Universidad de Valencia - CSIC, Valencia, Spain
- 176 Department of Physics, University of British Columbia, Vancouver, BC, Canada
- 177 Department of Physics and Astronomy, University of Victoria, Victoria, BC, Canada
- 178 Fakultät für Physik und Astronomie, Julius-Maximilians-Universität Würzburg, Würzburg, Germany

- 179 Department of Physics, University of Warwick, Coventry, UK
- 180 Waseda University, Tokyo, Japan
- 181 Department of Particle Physics and Astrophysics, Weizmann Institute of Science, Rehovot, Israel
- 182 Department of Physics, University of Wisconsin, Madison, WI, USA
- 183 Fakultät für Mathematik und Naturwissenschaften, Fachgruppe Physik, Bergische Universität Wuppertal, Wuppertal, Germany
- 184 Department of Physics, Yale University, New Haven, CT, USA
- 185 Yerevan Physics Institute, Yerevan, Armenia
- ^a Also at Borough of Manhattan Community College, City University of New York, New York, NY, USA
- ^b Also at CERN, Geneva, Switzerland
- ^c Also at CPPM, Aix-Marseille Université, CNRS/IN2P3, Marseille, France
- ^d Also at Département de Physique Nucléaire et Corpusculaire, Université de Genève, Geneva, Switzerland
- ^e Also at Departament de Física de la Universitat Autònoma de Barcelona, Barcelona, Spain
- ^f Also at Departamento de Física, Instituto Superior Técnico, Universidade de Lisboa, Lisboa, Portugal
- ^g Also at Department of Applied Physics and Astronomy, University of Sharjah, Sharjah, United Arab Emirates
- ^h Also at Department of Financial and Management Engineering, University of the Aegean, Chios, Greece
- ⁱ Also at Department of Physics and Astronomy, Michigan State University, East Lansing, MI, USA
- ^j Also at Department of Physics and Astronomy, University of Louisville, Louisville, KY, USA
- ^k Also at Department of Physics, Ben Gurion University of the Negev, Beer Sheva, Israel
- ^l Also at Department of Physics, California State University, East Bay, USA
- ^m Also at Department of Physics, California State University, Fresno, USA
- ⁿ Also at Department of Physics, California State University, Sacramento, USA
- ^o Also at Department of Physics, King's College London, London, UK
- ^p Also at Department of Physics, St. Petersburg State Polytechnical University, St. Petersburg, Russia
- ^q Also at Department of Physics, Stanford University, Stanford, CA, USA
- ^r Also at Department of Physics, University of Adelaide, Adelaide, Australia
- ^s Also at Department of Physics, University of Fribourg, Fribourg, Switzerland
- ^t Also at Department of Physics, University of Michigan, Ann Arbor, MI, USA
- ^u Also at Dipartimento di Matematica, Informatica e Fisica, Università di Udine, Udine, Italy
- ^v Also at Faculty of Physics, M.V. Lomonosov Moscow State University, Moscow, Russia
- ^w Also at Giresun University, Faculty of Engineering, Giresun, Turkey
- ^x Also at Graduate School of Science, Osaka University, Osaka, Japan
- ^y Also at Hellenic Open University, Patras, Greece
- ^z Also at IJCLab, Université Paris-Saclay, CNRS/IN2P3, 91405, Orsay, France
- ^{aa} Also at Institutio Catalana de Recerca i Estudis Avancats, ICREA, Barcelona, Spain
- ^{ab} Also at Institut für Experimentalphysik, Universität Hamburg, Hamburg, Germany
- ^{ac} Also at Institute for Mathematics, Astrophysics and Particle Physics, Radboud University Nijmegen/Nikhef, Nijmegen, Netherlands
- ^{ad} Also at Institute for Nuclear Research and Nuclear Energy (INRNE) of the Bulgarian Academy of Sciences, Sofia, Bulgaria
- ^{ae} Also at Institute for Particle and Nuclear Physics, Wigner Research Centre for Physics, Budapest, Hungary
- ^{af} Also at Institute of Particle Physics (IPP), Waterloo, Canada
- ^{ag} Also at Institute of Physics, Academia Sinica, Taipei, Taiwan
- ^{ah} Also at Institute of Physics, Azerbaijan Academy of Sciences, Baku, Azerbaijan
- ^{ai} Also at Institute of Theoretical Physics, Ilia State University, Tbilisi, Georgia
- ^{aj} Also at Instituto de Física Teórica, IFT-UAM/CSIC, Madrid, Spain
- ^{ak} Also at Istanbul University, Dept. of Physics, Istanbul, Turkey
- ^{al} Also at Joint Institute for Nuclear Research, Dubna, Russia
- ^{am} Also at Louisiana Tech University, Ruston, LA, USA
- ^{an} Also at LPNHE, Sorbonne Université, Université de Paris, CNRS/IN2P3, Paris, France
- ^{ao} Also at Manhattan College, New York, NY, USA
- ^{ap} Also at Moscow Institute of Physics and Technology State University, Dolgoprudny, Russia

^{aq} Also at National Research Nuclear University MEPhI, Moscow, Russia

^{ar} Also at Physics Department, An-Najah National University, Nablus, Palestine

^{as} Also at Physics Dept, University of South Africa, Pretoria, South Africa

^{at} Also at Physikalisches Institut, Albert-Ludwigs-Universität Freiburg, Freiburg, Germany

^{au} Also at School of Physics, Sun Yat-sen University, Guangzhou, China

^{av} Also at The City College of New York, New York, NY, USA

^{aw} Also at The Collaborative Innovation Center of Quantum Matter (CICQM), Beijing, China

^{ax} Also at TRIUMF, Vancouver, BC, Canada

^{ay} Also at Università di Napoli Parthenope, Naples, Italy

* Deceased